scientific reports

Check for updates

OPEN

Integrated in vitro, in silico, and in vivo approaches to elucidate the antidiabetic mechanisms of *Cicer arietinum* and *Hordeum vulgare* extract and secondary metabolites

Asif Shahzad[1,2,4], Wenjing Liu[1,4], Shoukat Hussain[2,4], Yueli Ni[1,4], Kun Cui[1], Yijian Sun[1], Xiangjie Liu[1], Qiuxin Duan[1], Jiaojiao Xia[1], Jinshan Zhang[1], Zhe Xu[1], Buqing Sai[1], Yuechun Zhu[1], Qiao Zhang[1]✉ & Zhe Yang[3]✉

Diabetes mellitus is a group of metabolic disorders that can lead to severe health problems, and the current treatments often have harmful side effects. Therefore, there is a growing interest in discovering new antidiabetic drugs with fewer adverse effects, and natural products are a promising source for this purpose. *Cicer arietinum* and *Hordeum vulgare* are plants with high levels of phytochemicals that have been shown to have therapeutic properties. This study investigates the anti-diabetic potential of *C. arietinum* and *H. vulgare* seeds and their secondary metabolites. We employed a comprehensive approach combining in vitro, in silico, and in vivo methods to evaluate the efficacy of the compounds. Our findings reveal that the extracts of *C. arietinum* (IC_{50} 55.08 µg/mL) and *H. vulgare* (IC_{50} 115.8 ± 5 µg/mL) demonstrated a stronger inhibitory effect on α-amylase compared to acarbose (standard drug) (IC_{50} 196.3 ± 10 µg/mL). Similarly, both *C. arietinum* and *H. vulgare* exhibited significant inhibitory activity against α-glucosidase (IC_{50} 100.2 ± 5 µg/mL and IC_{50} 216.2 ± 5 µg/mL, respectively) compared to acarbose (IC_{50} 246.5 ± 10 µg/mL). To further investigate their mechanism of action, a computational screening of 194 phytochemicals from these plants was conducted, followed by molecular docking with α-amylase (PDB ID#1B2Y) and α-Glucosidase (PDB ID# 5NN8) receptors. According to the binding affinities and molecular dynamics (MD) simulations, Medicagol, Euphol, Stigmasterol, and Beta-Sitosterol emerged as promising candidates for diabetes treatment. Molecular dynamics showed that Medicagol was a strong inhibitor against selected receptor proteins because the ligand–protein complexes remained stabilized during the entire simulation time of 100 ns. In vitro analysis also confirmed that Medicagol, stigmasterol, and Euphol have significant potential for type 2 diabetes prevention via inhibition of carbohydrates hydrolyzing enzymes. In vivo study demonstrated significant therapeutic effects in STZ-induced diabetes mice. Including reductions in hyperlipidemia, hyperglycemia, and insulin resistance. Histopathological analysis revealed that plant extracts mitigated STZ-induced pancreatic and liver damage. Additionally, extracts enhanced antioxidant defenses by increasing SOD, CAT, and GSH levels, while decreasing MDA levels in the liver, kidneys, and pancreas, highlighting their protective role against oxidative stress. These results support the potential of *Cicer arietinum* and *Hordeum vulgare* as natural sources for developing antidiabetic agents.

Keywords Diabetes mellitus, Docking studies, Phytochemicals, Molecular dynamics simulations, Medicagol, Druggability, STZ-induced mice, Hepatoprotective effect

[1]Department of Biochemistry and Molecular Biology, School of Basic Medical Sciences, Kunming Medical University, 1168 Yuhua Road, Chenggong, Kunming 650500, Yunnan, People's Republic of China. [2]Departments of Biochemistry, Government College University Faisalabad, Faisalabad 38000, Pakistan. [3]Departments of Pathology, The First Affiliated Hospital of Kunming Medical University, 295 Xichang Road, Wuhua, , Kunming 650032, Yunnan, People's Republic of China. [4]Asif Shahzad, Wenjing Liu, Shoukat Hussain and Yueli Ni contributed equally to this work. ✉email: zhangqiao200824@126.com; zyangpku@163.com

Diabetes mellitus (DM) is a rapidly growing metabolic condition identified by continual high blood sugar levels[1,2]. It has been projected that by 2025, approximately 455 million individuals worldwide will be affected by diabetes. Estimates suggest that by 2045, the population afflicted with diabetes could rise to 693 million[3]. The primary consequence of DM is elevated blood sugar levels, which occur as a result of inadequate insulin production or the malfunction of pancreatic beta cells responsible for insulin production[4]. Chronic hyperglycemia associated with diabetes can lead to chronic harm, impaired function, and eventual organ failure of multiple systems, encompassing the eyes, kidneys, nerves, heart, and blood vessels. To address this, one approach is to inhibit the activity of enzymes such as α-glucosidase & α-amylase which are involved in carbohydrate digestion[5]. Several medications taken orally to address high blood sugar levels, including sulfonylureas, glucosidase inhibitors, and amylase inhibitors, have been recognized for their ability to improve glycemic control[6]. Inhibitors targeting α-glucosidase and α-amylase, such as miglitol and acarbose exert dose-dependent effects by impeding the conversion of complex polysaccharides into simpler sugars within the intestines[7]. Inhibitors of α-amylase and α-glucosidase are therapeutic targets for managing postprandial hyperglycemia in diabetic patients. By delaying carbohydrate digestion and absorption, these inhibitors help maintain blood glucose levels within a normal range. While efficacious in managing postprandial hyperglycemia, these agents lack specificity for particular sites and may induce adverse effects including bloating, flatulence, nausea, and gastroenteritis[8,9]. Current treatments for diabetes, including insulin therapy and oral hypoglycemic agents are often accompanied by adverse effects and limitations such as hypoglycemia, weight gain, and drug resistance[10]. Recent studies have demonstrated the effectiveness of natural α-amylase and α-glucosidase inhibitors from various plant sources in controlling blood sugar levels. Phytochemicals derived from plants notably flavonoids, have emerged as promising candidates due to their ability to inhibit α-amylase and α-glucosidase[11–13]. This inhibition mechanism offers a promising avenue for blood glucose level management.

In recent years, there has been growing interest in the potential of natural products for managing diabetes due to their efficacy, safety, and minimal side effects[14]. Among these, chickpeas (*C. arietinum*), play a crucial role in the diets of millions worldwide, providing protein and minerals. Chickpeas are widely consumed and are among the most popular pulses globally[15]. Several components found in chickpeas have demonstrated various health benefits in both preclinical and clinical studies[16], including antioxidant[17], antifungal[18], and anti-inflammatory properties[19]. Recent research has highlighted the presence of bioactive compounds such as flavonoids, saponins, and phenolic acids in chickpeas, which exhibit significant inhibitory activity against α-amylase and α-glucosidase. It was demonstrated that chickpea extracts significantly reduced postprandial blood glucose levels in diabetic rat models through enzyme inhibition[20]. Barley (*H. vulgare*), a member of the Poaceae family and the Triticeae tribe, is ranked as the fourth most significant stable food globally, following wheat, rice, and maize[21,22]. It is easily accessible and economically viable in numerous regions across the globe. Barley is rich in dietary fiber, particularly β-glucan, which has been associated with various metabolic disorders, including diabetes, making it a beneficial nutritional component and improving glycemic control[23]. Additionally, *H. vulgare* is among the 300 plant species commonly used in Chinese herbal medicine[24]. Apart from its nutritional value, barley contains significant levels of biologically active substances like bioflavonoids, which have the potential to benefit human health[25,26]. Studies combining these approaches have provided deeper insights into the molecular mechanisms underlying the antidiabetic effects of plant extracts and their phytochemicals[27,28]. These seeds exhibit a variety of functions such as antimicrobial[29], hypolipidemic[30], anti-inflammatory[31], anti-ulcerogenic[32], gastroprotective[33], immunomodulatory[34], and antioxidant properties[35], among others. *C. arietinum* and *H. vulgare* seeds have a rich historical legacy of traditional practice for promoting health and wellness in the traditional healing system of Ayurveda, Unani, and Chinese herbal medicine. In recent years, the powdered form of these seeds has gained popularity in Pakistan for managing diabetes[36]. While there have been some investigations into the medicinal properties of *C. arietinum* (chickpeas) and *H. vulgare* (barley)[37,38], the available research on these natural products remains limited[14]. Hence, the present study aimed to investigate the anti-diabetic potential of *C. arietinum* and *H. vulgare* extracts and their secondary metabolites using both in vitro and in silico methods. Additionally, plant extracts are used in the in vivo study to investigate the antidiabetic potential against STZ-induced diabetic mice. The term in vitro refers to experiments conducted outside a living organism, typically in a controlled laboratory environment. In our study, in vitro methods were used to evaluate the antidiabetic properties of the plant extract by measuring their ability to inhibit the enzymes alpha-amylase and alpha-glucosidases. The term in silico refers to experiments conducted using computer simulations and computational techniques. In our study, in silico methods involved molecular docking studies to predict the interactions between the bioactive compounds identified in the plant extracts and the target enzymes. These simulations help in understanding the binding affinities and modes of interaction, providing insights into the potential mechanisms of action of the compounds. By exploring the inhibitory effects of key enzymes involved in carbohydrate metabolism and the interaction of their bioactive compounds with diabetic enzymes, we seek to elucidate the mechanisms underlying their anti-diabetic properties. Methanolic extracts of these medicinal plant seeds and evaluated their effects on the α-amylase and α-glucosidase enzymes, which play a role in diabetes management. Despite previous studies exploring the anti-diabetic potential of *C. arietinum and H. vulgare*, a comprehensive investigation into the specific secondary metabolites responsible for their anti-diabetic activity and potential mechanisms has not been conducted. Thus, this study aimed to investigate the binding efficiency of the secondary metabolites present in these seeds against the target proteins through *in-silico* techniques, including molecular docking, drug scan, ADMET analysis, and MD simulation.

Material and methods

Chemicals and reagents

All enzymatic assay kits and chemicals for in vitro and in vivo studies were purchased from Global Scientific, Lahore. Some chemicals/reagents were purchased from Sigma-Aldrich like p-nitrophenyl- α-G-Glucopyranoside

(p-NPG), Acrabose, soluble starch, 3,5-dinitro salicylic acid (DNS), Sodium carbonate (Na_2CO_3), hydrochloric acid (HCl), sodium hydroxide (NaOH), Sodium potassium tartrate, Sodium dihydrogen phosphate, Dimethyl sulfoxide (DMSO), Di-sodium hydrogen phosphate, and absolute methanol (37%).

Collection of plant sample

The mature and dry seeds of *C. arietinum* & *H. vulgare* were purchased from the local market of Faisalabad, Punjab, Pakistan. Authentication of these seeds was done by the taxonomist Department of Botany, Government College University in Faisalabad (GCUF), Punjab, Pakistan.

Extraction procedure

The collected plant materials were washed thoroughly with distilled water to remove impurities and air-dried at room temperature for three days. The dried samples were then ground into fine powder using a mechanical grinder. For *C. arietinum* extracts, 10 g of the powdered sample was subjected to Soxhlet extraction using 150 ml of absolute methanol as solvent using the modified methodology Kadan et al.[39]. The extraction process was carried out at 60 °C for 8 h. The extract was filtered using Whatman No. 1 filter paper and concentrated under reduced pressure using a rotary evaporator at 40 °C and a yield of 1.05 g (10.5%). To ensure consistency and reproducibility each batch of plant extract was performed in triplicate. The concentration extract was then lyophilized to obtain a dry powder, stored at − 20 °C until further analysis. For *H. vulgare* extracts, a similar procedure was followed with 10 g of the powdered sample extracted using 150 ml of absolute methanol. The extract was concentrated and lyophilized as described above.

In vitro assay

The α-amylase inhibition assay

An Inhibition assay of the α-amylase against plant extract was done using Adisakwattana et al.'s reported methods[40]. Briefly, 5 ml of plant extract (1.0 mg/ml) was mixed with 5 ml of α-amylase solution (5 U/ml in 0.1 M Sodium phosphate Buffer, pH 6.9) and incubated at 25 °C for 10 min. After incubation, 5 ml of 1% starch solution was added, and the mixture was incubated at 25 °C for an additional 10 min. The reaction was terminated by adding 1 ml of DNS reagent (3,5-dinitrosalicylic acid) and boiling the mixture for 5 min. Optical Density (OD) was measured at 540 nm by using a spectrophotometer. The α-amylase activity was validated using a standard curve of maltose, prepared by hydrolyzing a known starch concentration under assay conditions. The linearity of the assay was confirmed and the precision was assessed by performing the assay in triplicate. Acarbose (0.9 mg/ml) was used as a positive control due to its well-documented α-amylase inhibitory activity. A reaction mixture without the drug candidates was used as a negative control to establish baseline enzyme activity. The following equation was used to determine the inhibitory potential of α-amylase:

$$\alpha \text{ - amylase inhibition } = \frac{[\text{ABS blank} - \text{ABS test}]}{[\text{ABS blank}]} \times 100$$

The α-glucosidase inhibition assay

The α-Glucosidase inhibition assay was done by using the reported method of Kim et al.[41]. In brief, 5 ml of the plant extract (1.0 mg/ml) was mixed with 5 ml of α-glucosidase solution (5 U/ml in 0.1 M Potassium phosphate buffer, pH 6.8) and incubated at 37% for 15 min. The reaction was initiated by adding 5 ml of 20 mM p-nitrophenyl-α-D-glucopyranoside (pNPG) solution and incubating at 37% for 20 min. The reaction was terminated by adding 10 ml of 0.1 M Na_2CO_3. Optical Density (OD) was measured at 540 nm by using a spectrophotometer. The α-glucosidase activity was validated using a standard curve of p-nitrophenol, generated by hydrolyzing a known concentration of pNPG under assay conditions. The linearity of the assay was confirmed and the precision was assessed by performing the assay in triplicate. Acarbose (0.9 mg/ml) was used as a positive control due to its well-documented α-amylase inhibitory activity. A reaction mixture without the drug candidates was used as a negative control to establish baseline enzyme activity. The following equation was used to determine the intestinal-glucosidase enzyme's inhibitory potential;

$$\alpha \text{ - Glucosidase inhibition } = \frac{[\text{ABS blank} - \text{ABS test}]}{[\text{ABS blank}]} \times 100$$

In silico analysis

Screening of bioactive compound

For the current study, a total of 194 biologically active phytochemicals from *C. arietinum* and *H. vulgare* were retrieved that may show anti-diabetic activity through the database IMPPAT (https://cb.imsc.res.in/imppat/)[42] and TCMSP (https://tcmsp-e.com/tcmsp.php)[43] (normal pharmacological analysis tools that help to find new drugs from herbal medicines). The structure of phytochemicals was retrieved from PubChem (https://pubchem.ncbi.nlm.nih.gov/)[44] in the SDF format of each phytochemical.

Target protein retrieval

For the current study two target proteins were selected α-amylase (PDB ID#1B2Y) & α-glucosidase (PDB ID# 5NN8), structures were obtained from the protein data bank (PDB) (https://www.rcsb.org/)[45] and their respective PDB format files were retrieved.

Preparation of receptor and ligand molecules
The three-dimensional structure of selected enzymes was retrieved from the protein data bank (PDB). The protein structures were prepared for docking by removing water molecules, adding hydrogen atoms, and optimizing the protonation states of amino acid residues at physiological pH using the Discovery Studio tool (v24.1.0.23298)[46]. The chemical structures of the phytochemicals identified in the plants were obtained from the PubChem database. The ligands were prepared for docking by minimizing their energy using the PyRx-virtual screening tool software. The ligands were converted into PDBQT format. Both the proteins and ligands were prepared and ready for further analysis in the docking studies.

Molecular docking
The secondary metabolites identified from the online database mentioned above were subjected to molecular docking studies to assess their binding affinities to α-amylase (PDB ID#1B2Y) & α-glucosidase (PDB ID# 5NN8) obtained from the Protein Data Bank (PDB). The molecular docking was performed using PyRx-virtual screening tool software. The docking grid was centered on the active site of the protein, and the grid box dimensions were set to encompass the binding pocket. The docking parameters were set to default values, and the docking simulations were performed with 10 runs of each ligand. The binding affinities and interaction were analyzed using the Discovery Studio tool (v24.1.0.23298). the docking protocol was validated by redocking the ligands from the PDB structures of α-amylase & α-glucosidase into their respective binding sites[47].

Drug scan
The drug scan of Biologically active phytochemicals was conducted using Lipinski's rule of five, (hydrogen bond acceptors ≤ **10**, hydrogen bond donor ≤ **5**, molecular weight ≤ **500**, molar refractivity 40–130 and Log P ≤ **5**) as proposed by Lipinski et al. in 1997, these properties were checked through the database SWISSADME (http://www.swissadme.ch/index.php). This rule evaluates various molecular properties of compounds to assess their drug-likeness. Phytochemicals that fulfill these five rules were considered favorable for further investigation, as they were less likely to have harmful effects on the body[48].

ADMET profiling
The best-docked phytochemicals were selected for ADMET (absorption, distribution, metabolism, elimination, and toxicity) profiling based on their binding affinities and interaction profiles obtained from the molecular studies. The main pharmacokinetic properties of these phytochemicals were predicted by the online tool admetSAR (http://lmmd.ecust.edu.cn/admetsar2)[49], pkCSM (https://biosig.lab.uq.edu.au/pkcsm/)[50] and ADMETlab (https://admetmesh.scbdd.com/)[51]. The calculation of Log P, a measure of a compound's lipophilicity, hydrophobicity, and polarity, was based on a formula that evaluates the compound's capacity to bind to hydrophobic regions on the target protein[50].

Molecular dynamic simulation analysis
Molecular dynamics (MD) simulations were used to assess the stability of docked ligand–protein complexes[52]. Complexes were chosen based on criteria such as minimum docking score, lowest RMSD, minimal Lipinski's Rule of violations (ideally zero or one), and druggability analysis. The Desmond Module within Schrodinger software was employed for MD simulations, utilizing a water-solvated solvent system. The TIP3P water model was selected to address simulation issues[53]. An orthorhombic simulation box with periodic boundary conditions and a 10 Å buffer distance from the protein's outer surface was utilized. A 0.15 M NaCl solution was added to maintain osmotic equilibrium and counter ions were added to neutralize the system, before production MD runs an equilibration process was executed, and the simulations were conducted at 1.013 bar pressure and 310 K temperature each spanning 100 ns and generating 100 frames in the trajectory. Simulation interactions were analyzed using a simulation interaction diagram[54].

Animal experimental study

Induction of DB
The in vivo study was conducted using Swiss mice aged 5 to 9 weeks, with an average weight of 26 ± 2 g, maintained at an ambient temperature of 25 ± 2 ℃, and provided standard food and ad libitum water[55]. Diabetes was induced in the mice via a single intraperitoneal injection of streptozotocin (STZ) at a dosage of 3 mg per 26 g of the body weight, delivered in a citrate buffer at pH 4.5[56]. This administration resulted in a diabetic state after 7 days, with blood glucose levels reaching approximately 200 to 250 mg/dl. All procedures followed the guidelines established by the Institutional Animal Ethical Committee.

Treatment with plant extract
Plant extracts (*C. arietinum* (5.5 mg/g) & *H. vulgare* (11.6 mg/g) and standard drug acarbose (10.8 mg/g) based on the previous analysis) reconstituted in distilled water with 0.5% dimethyl sulfoxide (DMSO) were administered intraperitoneally to the experimental mice for 21 days. Each group comprised six animals, with the non-diabetic control and diabetic control groups receiving only the vehicle (distilled water + 0.5% DMSO). After 21 days of treatment, the animals were sacrificed, and their organs were excised, washed with phosphate-buffered saline (PBS), and stored at − 20 ℃ for further analysis.

Fasting blood glucose levels
Fasting blood glucose levels were monitored periodically during the treatment using the tail prick method with an Accu-Check Active glucometer [57]. Blood glucose concentrations were recorded in milligrams per deciliter.

Oral glucose tolerance test (OGTT)
The oral glucose tolerance test was conducted on overnight fasted normal, diabetic, and treated mice on the 21st day of the treatment. Glucose (2 g/kg body weight) was administered orally, and blood glucose levels were measured at 0, 30, 60, 90, and 120 min post-administered glucose [58].

Pancreatic and intestinal glucosidase activity
The mice were sacrificed after 21 days of treatment. Pancreatic and small intestinal tissues were homogenized in 10 mM Phosphate buffer saline (PBS) containing 100 mM NaCl and a protease inhibitor cocktail. The homogenates were then centrifuged, and the supernatant was utilized as the source of enzyme activity. Glucosidase activity was assessed using the dinitrosalicylic acid (DNSA) method[59].

G6PD activity
G6PD activity was assessed using the methodology of Jayachandran[60], post-treatment liver tissue was homogenized in 10 mM phosphate buffered saline (PBS). The change in absorbance of the reaction mixture, which contained 1 M tris-chloride buffer, 25 mM glucose-6-phosphate, 0.2 M magnesium chloride, 2 mM NADP, and homogenized tissue, was measured at 340 nm for 10 min. One unit of enzyme activity was defined as the amount that catalyzed the reduction of 1 µM NADP per minute.

Glycogen estimation
Glycogen levels were estimated in liver and muscle tissues post-treatment[61]. The tissues were homogenized in warm ethanol and centrifuged. The residue was dried and dissolved in distilled water with perchloric acid for extraction. This mixture was then centrifuged, and the supernatant was analyzed for glucose concentration using the phenol–sulfuric acid method at 490 nm. The amount of glycogen in the tissue sample was expressed as micrograms of glucose per milliliter of tissue extract.

Biochemical analysis
The liver function markers (Aspartate aminotransferase (AST), Alanine aminotransferase (ALT), alkaline phosphatase (ALP), and total bilirubin), renal function makers (Urea and creatinine), and lipid profile components (triglycerides (TG), total cholesterol (TC), high-density lipoprotein (HDL), low-density lipoprotein (LDL), and very low-density lipoprotein (VLDL) were measured according to the instructions provided by standard commercial kits[62].

Oxidative stress biomarkers
The oxidative stress (OS) parameters were estimated using the previously described method[63]. Ten percent (w/v) of tissue homogenates of the dissected organs were prepared in ice-cold phosphate-buffered saline (PBS). The homogenates were centrifuged at 1500 g for 15 min at 4℃, and the supernatants were collected and stored at −20℃ for further analysis. Protein content in the homogenates was measured using the Lowry method, with bovine serum albumin as the standard.

Superoxide dismutase activity (SOD) SOD regulates reactive oxygen species (ROS) levels by converting superoxide into hydrogen peroxide and oxygen. SOD activity was determined using the pyrogallol method, where absorbance was measured at 325 nm at intervals of 0.5 min over a total duration of 5 min.

Catalase activity (CAT) Catalase catalyzes the degradation of hydrogen peroxide into water and oxygen. To assess CAT activity in tissues, a spectrophotometric method based on the degradation of hydrogen peroxide was employed, measuring absorbance at 240 nm at 0.35-min intervals for three measurements as previously described.

Reduced glutathione (GSH) GSH levels were assessed using the previously described method. Equal volumes (1 ml) of tissue sample and trichloroacetic acid (TCA) were mixed with 4 ml of PBS (pH 7.4), followed by the addition of 500 µl of DNTB reagent. Absorbance was measured at 412 nm and expressed as micrograms per milligram.

Malondialdehyde (MDA) As outlined in previous procedures, MDA levels were determined using the thiobarbituric acid (TBA) method. The absorbance of the reactant mixture was measured at 532 nm and MDA concentration was expressed as nM/ml.

Histopathology
The animals were euthanized under ether anesthesia followed by cervical dislocation[64]. The liver and pancreas were carefully excised, promptly rinsed with ice-cold isotonic saline, and blotted on ash-free filter paper. The tissues were immediately prepared for histopathological analysis. Processing included fixation, dehydration, clearing, embedding in paraffin wax, and block preparation. Sections were cut using a rotary microtome to obtain slices of 5 µm thickness, which were subsequently stained with hematoxylin and eosin (H & E) and mounted on slides for microscopic examination.

Results

In vitro inhibitory activity of carbohydrate metabolizing enzymes by plant extract

The anti-diabetic properties of *C. arietinum* and *H. vulgare* methanol extracts were evaluated by measuring their inhibitory effects on pancreatic amylase and glucosidase, in comparison to the inhibitory drug, acarbose

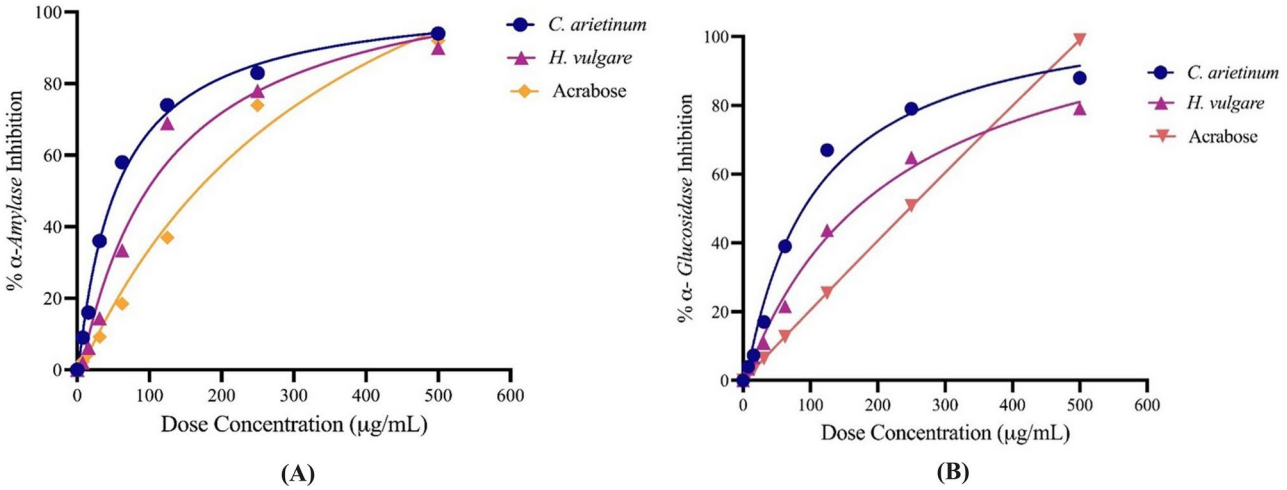

Fig. 1. The percentage inhibition of (**A**) α-amylase by increasing concentrations of *C. arietinum* and *H. vulgare*. The resulting IC50 are 55.08 ± 5 µg/mL and 115.8 ± 5 µg/mL respectively. (**B**) α-glucosidase by increasing concentrations of *C. arietinum* and *H. vulgare*. The resulting IC50 are 100.2 ± 5 µg/mL and 216.2 ± 5 µg/mL respectively.

Enzymes	*C. arietinum (Extract)*	*H. vulgare* (Extract)	Acarbose (Positive control)
α-Glucosidase	100.2 ± 5 µg/mL	216.2 ± 5 µg/mL	246.5 ± 10 µg/mL
α-amylase	55.08 ± 5 µg/mL	115.8 ± 5 µg/mL	196.3 ± 10 µg/mL

Table 1. The IC_{50} values of *C. arietinum* and *H. vulgare* for α-glucosidase and α-amylase.

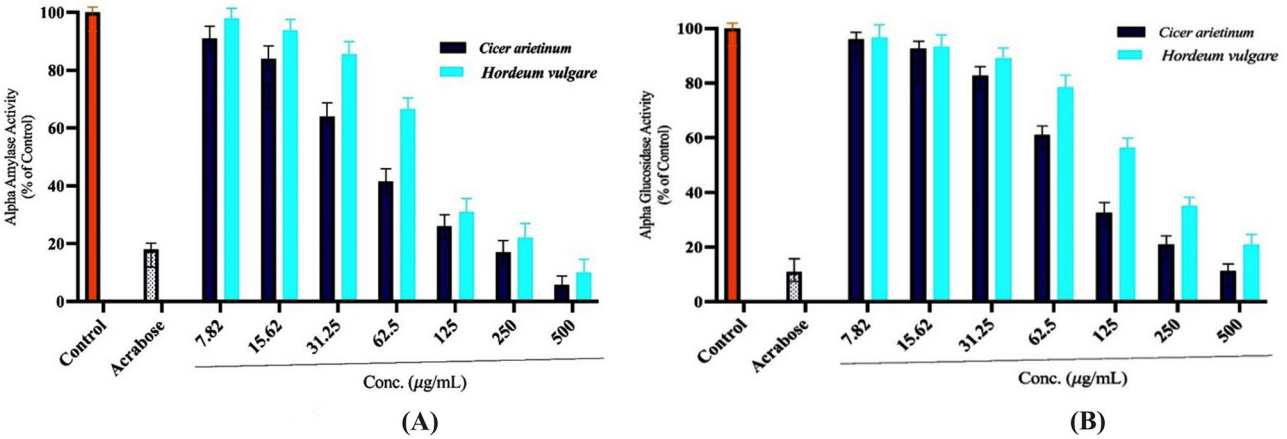

Fig. 2. Inhibition effects of *C. arietinum* and *H. vulgare* with positive control (Acrabose) and negative control (mixture without drug candidates) on (**A**) α-amylase (**B**) and α-glucosidase. This data was taken in triplicates (n = 3) with SD ± mean values.

was used. The results showed that both plant extracts inhibited alpha-amylase in a dose-dependent manner, with IC_{50} values of 55.08 and 115.8 g/mL for *C. arietinum* and *H. vulgare*, respectively (Fig. 1A, Table 1). Furthermore, both extracts also inhibited alpha-glucosidase, although to a lesser extent than alpha-amylase, with corresponding IC_{50} values of 100.25 g/mL and 216.25 g/mL for *C. arietinum* and *H. vulgare*, respectively (Fig. 1B, Table 1). The findings from the in vitro assessment were reliable with the results obtained from the docking experiment (Fig. 2).

In-silico analysis of receptor and ligand preparation

According to the results above, the potential of *C. arietinum* and *H. vulgare* for α-glucosidase and α-amylase inhibitory was preliminarily determined. In further investigation, the mechanism and molecular characteristics

Phytochemicals	PubChem ID	Binding affinity (kcal/mol) With 1B2Y	Binding affinity (kcal/mol) With 5NN8	Interacting amino acids with 1B2Y	Interacting amino acids with 5NN8
Medicagol	5,319,322	− 8.4	− 8.7	His305, Leu165, Trp59, Gln63, Asp197, Glu233	Lys903, Glu281, Ala842, Gly828, Leu826, Ala704, Ile780, Cso938
Euphol	441,678	− 9.7	− 8.0	Trp59, Val107, Ile51, Asp300, Asp192, Glu233	Trp A: 126
Beta-Sitosterol	222,284	− 9	− 7.5	Ile A:51, Trp A:59, Leu A:162, Leu A:165, Ala A:198, His A: 201	Pro457, Phe506, phe414
Fucosterol	5,281,328	− 9.1	− 7.8	Leu165, Ile51, Trp59, Ala198, His201, Leu162	Ala93, Trp126, Ala97, Tyr140
Stigmasterol	5,280,794	− 9.1	− 7.8	Ala198, Glu237, His201, Leu162, Leu165, Trp59	Ala719, Val718, Glu721, Gln715, Leu712, Glu748, Tyr822, His708, Ala749, Ile823, Ile824, Gly855, Glu856, Arg854, Gln352, Lys348

Table 2. Top-rated phytochemicals interactions with receptors.

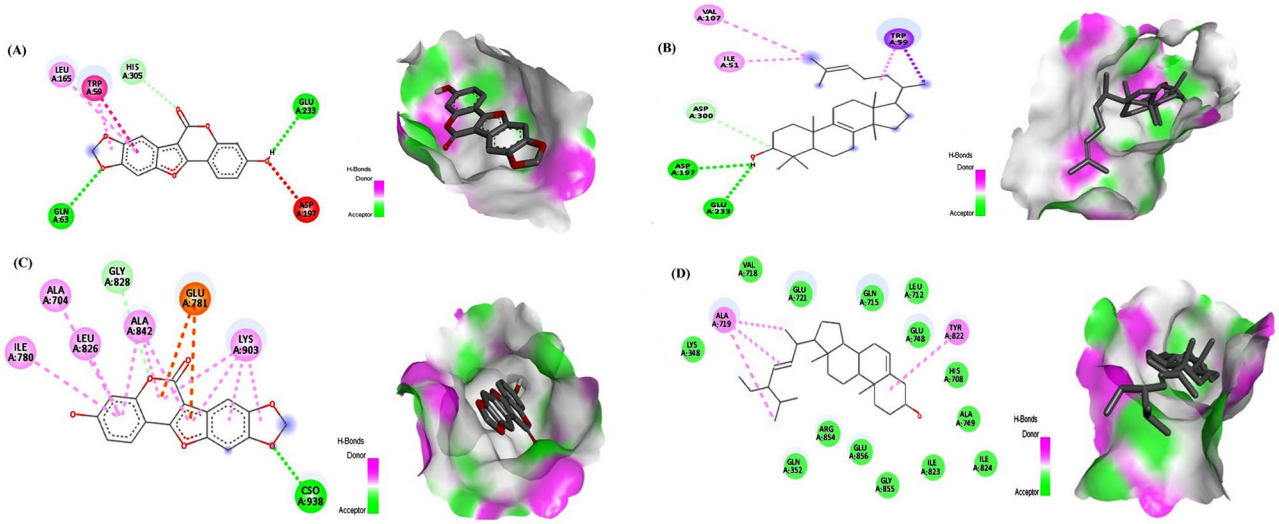

Fig. 3. Amino acid Interaction and pocket atom of phytochemicals against the receptors (**A**) Medicagol against α-amylase (1B2Y) and (**B**) Euphol against α-amylase (1B2Y) (**C**) Medicagol against α-glucosidase (5NN8) (**D**) Stigmasterol against α-glucosidase (5NN8).

were needed to clarify. Firstly, the in-silico analysis for the molecular interaction between ligands and receptors should be employed. Alpha amylase and alpha-glucosidase protein receptors' 3D structures were obtained from the protein data bank using their respective protein IDs of 1B2Y and 5NN8. All 194 phytochemicals employed as ligands were docked with specific target proteins for the development of new anti-diabetic drugs. Using Discovery Studio, the receptor was prepared by deleting additional chains, water molecules, ligand molecules, and heteroatoms. The prepared files were saved in the PDB format. The PyRx virtual screening software adds version was used to prepare the ligand molecules (3D confirmation), and the files were stored in the SDF format.

Molecular docking analysis

PyRx virtual screening tool and Bio-via discovery studio software were used to analyze the current investigation. The best confirmation of the ligand's binding to the protein is predicted by currently-in-use software. Top phytochemicals as drug candidate have been chosen based on binding affinity and RMSD values, and their interacting amino acids have been explained in Table 2. Each docking results were assigned one of nine conformation ratings based on the molecular docking investigations. The lowest binding affinity shows maximum interaction of the ligand molecules with the receptor's molecule. Top-rated phytochemicals, their binding interaction, and pocket atom visualization are expressed in Fig. 3A–D.

Pharmacological properties and ADMET profiling

Based on the molecular docking analysis results, the recommended phytochemicals were screened for possible drug candidates by the binding affinity score and probable interactions with the receptor's molecules. The drug-likeness character/Lipinski rule of five and ADMET profile were predicted for all compounds and are presented in Table 3. All phytoconstituents showed a positive drug-likeness score, and have high gastrointestinal absorption with HIA values > 90% and favorable Caco-2 cell permeability, indicating good oral bioavailability. The predicted skin permeability coefficients (log Kp) were within acceptable ranges, suggesting low dermal absorption which is beneficial for oral drug candidates. The predicted VDss values indicated moderate to high distribution volumes, suggesting extensive tissue distribution. however, none of the compounds showed significant BBB

Molecular properties							
Ligand	Molecular Mass (≤500 Dalton)	Hydrogen bond donor (≤5)	Hydrogen bond acceptor (≤10)	No. of rotatable Bond (≤10)	Log P (≤5)	Refractivity (40–130)	Violations
Medicagol	296.030	1	6	0	2.27	77.85	0
Euphol	426.390	1	1	4	7.74	137.04	1
beta-Sitosterol	414.390	1	1	6	7.19	133.23	1
Fucosterol	412.70	1	1	5	7.07	132.75	1
Stigmasterol	412.70	1	1	5	6.97	132.75	1

Table 3. The molecular and drug-likeliness properties of the top five phytochemicals were evaluated through Lipinski's Rule of Five (1B2y & 5NN8).

Phytochemicals	Medicagol	Euphol	Beta-Sitosterol	Fucosterol	Stigmasterol
Absorption and distribution					
BBB	No	Yes	Yes	Yes	Yes
HIA	Yes	Yes	Yes	Yes	Yes
Caco-2 Permeability	No	Yes	Yes	Yes	Yes
PGS	No	No	Yes	Yes	No
PGI	No	No	No	Yes	Yes
Metabolism					
CYP3A4 substrate	No	Yes	No	No	Yes
CYP2C9 substrate	No	No	No	No	No
CYP2D6 substrate	No	No	No	No	No
CYP3A4 inhibition	Yes	No	No	No	No
CYP2C9 inhibition	No	No	No	No	No
CYP2C19 inhibition	No	No	No	No	No
CYP2D6 inhibition	Yes	No	No	No	No
Toxicity					
AMES Toxicity	No	No	No	No	No
Carcinogens	No	No	No	No	No

Table 4. ADMET-related drug-like parameters of the best-selected phytochemicals; BBB: Blood–Brain Barrier; HIA: Human Intestinal Absorption; PGS: P-glycoprotein substrate; PGI: P-glycoprotein inhibitor; ROCT: Renal Organic Cation Transporter;

permeability, reducing the risk of central nervous system side effects. The ADMET analysis revealed that the selected phytochemicals have low to moderate potential for CYP450 enzyme inhibition, particularly CYP3A4 and CYP2D6 indicating a lower risk of metabolic drug-drug interaction. The predicted metabolic stability was acceptable for all compounds with moderate clearance rates. Renal clearance predictions indicated that the compounds are likely to be efficiently excreted via the kidney, reducing the risk of accumulation and potential toxicity. None of the selected phytochemicals were predicted to be mutagenic in the Ames test, and all showed low hepatotoxicity and carcinogenicity risks. the overall ADMET profile is represented in Table 4**.** Overall, the results are satisfactory, and the compound can be used as a potential drug candidate because selected phytochemicals were determined to be nontoxic and non-carcinogenic.

Molecular dynamics simulation analysis

The trajectories obtained from the MD simulations were analyzed using Desmond Module within Schrodinger software and visualized with visual molecular dynamics software. The RMSD of the protein backbone and ligand was calculated to assess the stability of the complexes over 100 ns. The RMSF of the protein residues was calculated to identify regions with significant flexibility. The number and stability of hydrogen bonds between the ligands and protein residues were monitored throughout the simulation. Medicagol, Euphol, Beta-sitosterol, Fucosterol, and stigmasterol exhibited robust binding interactions with receptor proteins without violating Lipinski's rule of five. Notably, Medicagol demonstrated strong binding interactions with all selected receptor proteins, prompting its selection for MD simulation studies. The objective of the MD simulations was to elucidate the dynamic binding properties of these ligands within the binding pockets of target proteins. Schrodinger's Desmond Module facilitated the MD simulations to assess the stability of the protein–ligand complexes. During MD simulation of the Medicagol α-amylase protein complex (Fig. 4A), minor fluctuations in protein RMSD were initially observed increasing from 1.2 to 2.5 Å. However, the average protein RMSD change remained approximately 1.2 Å, indicating overall stability throughout the 100 ns simulations. Medicagol

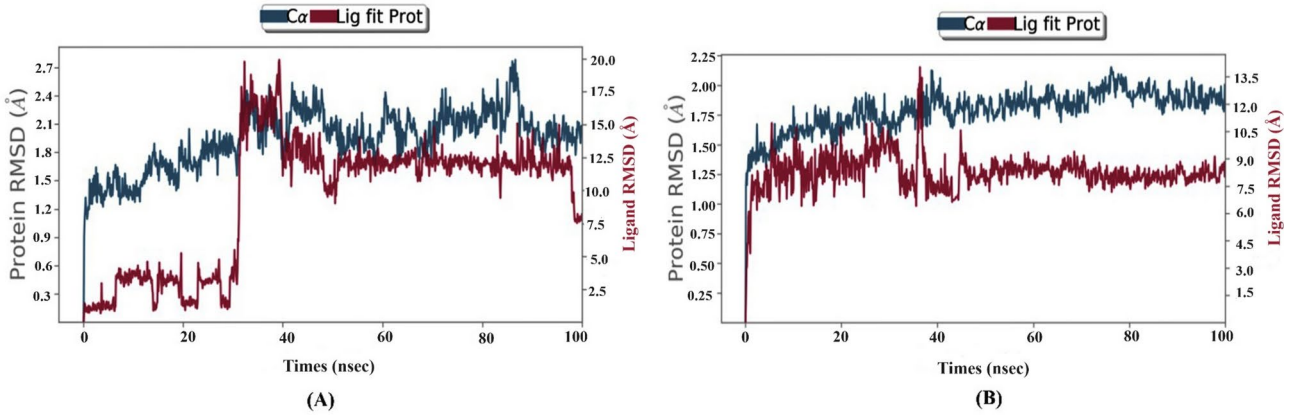

Fig. 4. Molecular Dynamics simulations were conducted, displaying root mean square deviation (RMSD) trajectories. The simulation spanned 100 ns at a pressure of 1.00314 bar, temperature of 310 K, and pH of 7.4, generating 1000 frames. The trajectories represent the MD simulation outcomes for the docked complexes of (**A**) Medicagol- α-amylase and (**B**) Medicagol- α-glucosidase. The blue line corresponds to the left y-axis, indicating the fluctuation of protein RMSD over time, while the red line corresponds to the right Y-axis representing the variation of Medicagol phytochemical RMSD over the simulation period.

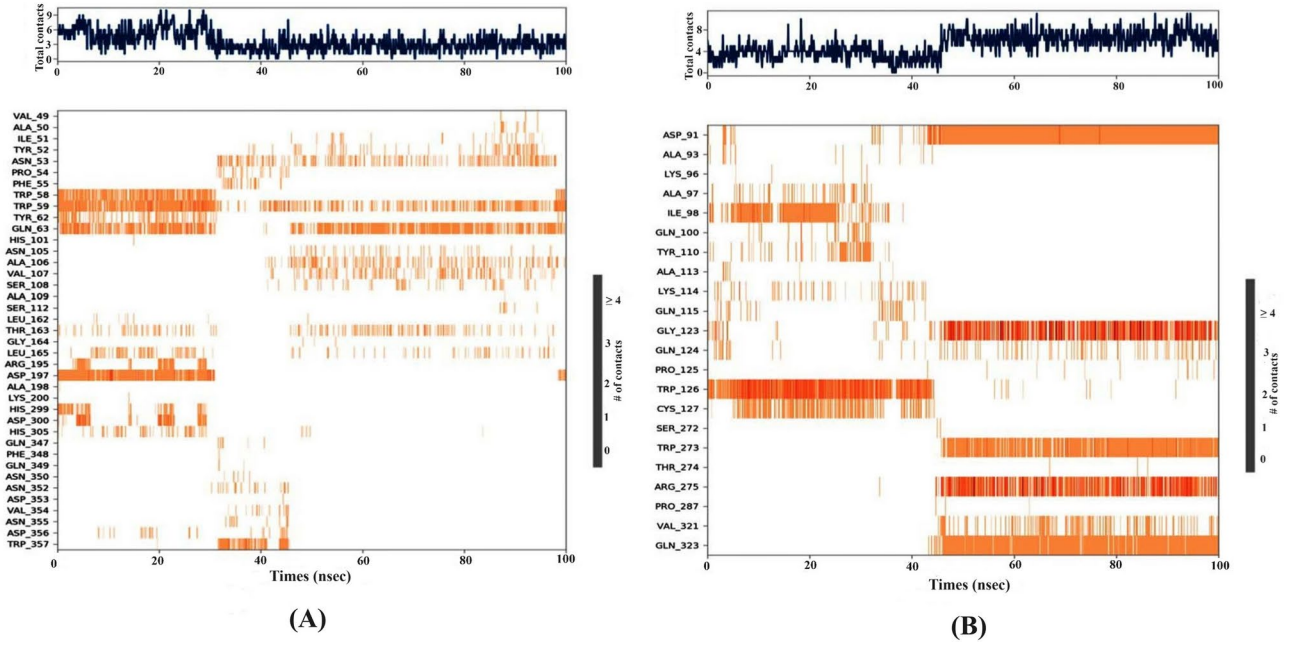

Fig. 5. Evaluate the consistency of hydrogen bond interaction stability between Medicagol and key residues of the (**A**) α-amylase protein and (**B**) α-glucosidase protein.

achieved stabilization after 34 ns and maintained a strong association with α-amylase throughout the simulation duration, the average change in the ligand RMSD was approximately 1.6 Å, which is within an acceptable range.

For the Medicagol- α-glucosidase protein complex (Fig. 4B), the mean protein backbone RMSD of α-glucosidase was approximately 1.25 Å, with acceptable changes up to 2.25 Å. Despite fluctuations observed in the ligand RMSD achieved stabilization after 4 ns and maintained a strong association with α-glucosidase. At 35 ns a mode shift occurred after which the ligand remained unstable until the end of the simulation. Overall trajectory analysis indicated ligand stability within the original pocket of α-glucosidase protein throughout the 100 ns simulation duration. The stability and consistency of hydrogen bond interactions, as well as the crucial amino acid residues within each receptor protein interacting with the selected phytochemical ligand, were assessed throughout the molecular dynamics (MD) simulation. The results depicted in Fig. 5A, B demonstrate that the ligand complexes with their respective proteins remain stable over the 100 ns simulation period, additionally, Root Mean Square Fluctuation (RMSF) analysis of Medicagol phytochemical complexed with the respective proteins (Fig. 6) revealed stable peaks, indicating consistent interactions with important amino

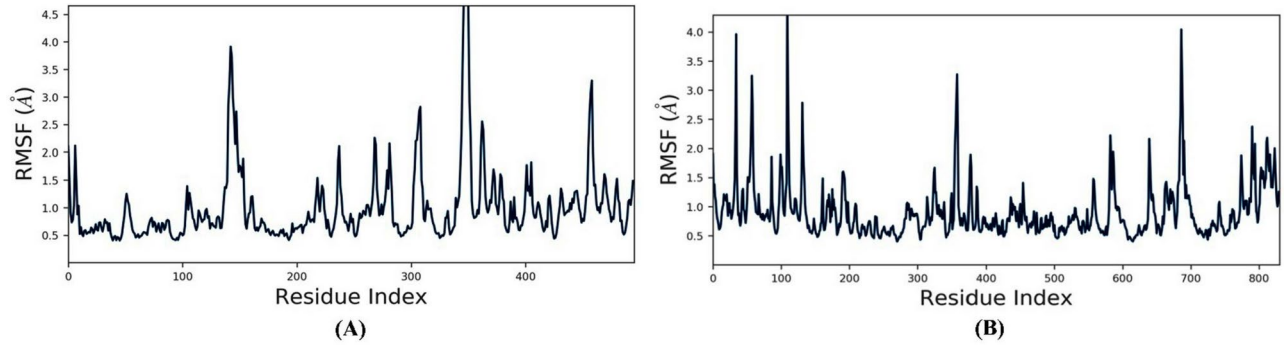

Fig. 6. The residue-wise Root Mean Square Fluctuation (RMSF) analysis was conducted over a 100 ns period for protein–ligand complexes involving Medicagol and two distinct proteins (**A**) α-amylase and (**B**) α-glucosidase. In the RMSF analysis, it was revealed negligible fluctuation in the interacting residues of the docked protein complexes.

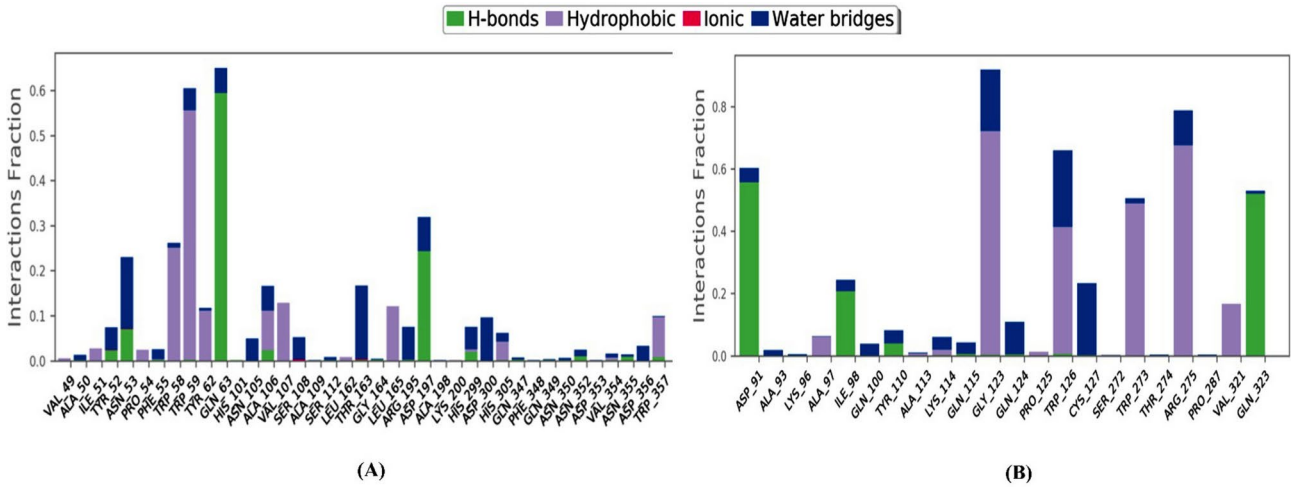

Fig. 7. Protein–ligand contact histogram. Protein structure complexed with the best phytochemical (**A**) α-amylase and (**B**) α-glucosidase.

acid residues throughout the simulation. These findings provide robust evidence for the stability of the selected phytochemicals complexed with their respective receptor proteins following molecular docking and MD simulation studies, suggesting their potential use in drug design for addressing diabetes. The Protein–Ligand Interaction Fingerprints (PLIF) analysis of α-amylase protein complexed with Medicagol, both Pre and Post MD simulation highlighted specific amino acids crucial for complex stabilization in drug design shown in Fig. 7. Notably, Tyr 52, Asn 53, Gln 63, Ala 106, Asp 197, His 299, Asn 352, and Asn 355 were identified as key residues forming hydrogen bonds with the ligand. Additionally, Ile 51, Pro 54, Trp58, Trp 59, Tyr 62, Ala 106, Leu 165, His 305, and Trp 357 were implicated in significant hydrophobic interactions with the ligand (Fig. 7A). In the α-glucosidase protein complex with Medicagol, PLIF analysis indicated the significance of amino acids Asp 91, Ile 98, Tyr 110, and Gln 323 in forming hydrogen bonds with Medicagol for complex stability. Furthermore, Ala 97, Lys 114, Gly 123, Pro 125, Trp 126, Trp 273, Ard 275, and Val 321 were identified as crucial residues involved in hydrophobic interactions (Fig. 7B).

In vitro inhibitory activity of carbohydrate metabolizing enzymes by phytochemicals

In vitro inhibitory activity of α-amylase

The inhibitory potencies of top selected phytochemicals from in silico study on α-amylase activity (Fig. 8A). As expected, acarbose showed the lowest inhibition establishing its relative potency as an amylase inhibitor. Euphol also was a strong inhibitor of α-amylase, exhibiting a high significance with 95% CI, p value <0.01, Medicagol was also a strong inhibitor of α-amylase but their inhibition result was statistically significant with 95% CI, p value <0.05. These data indicate that Euphol and Medicagol are as potent and efficient as the drug, acarbose, in inhibiting α-amylase activity.

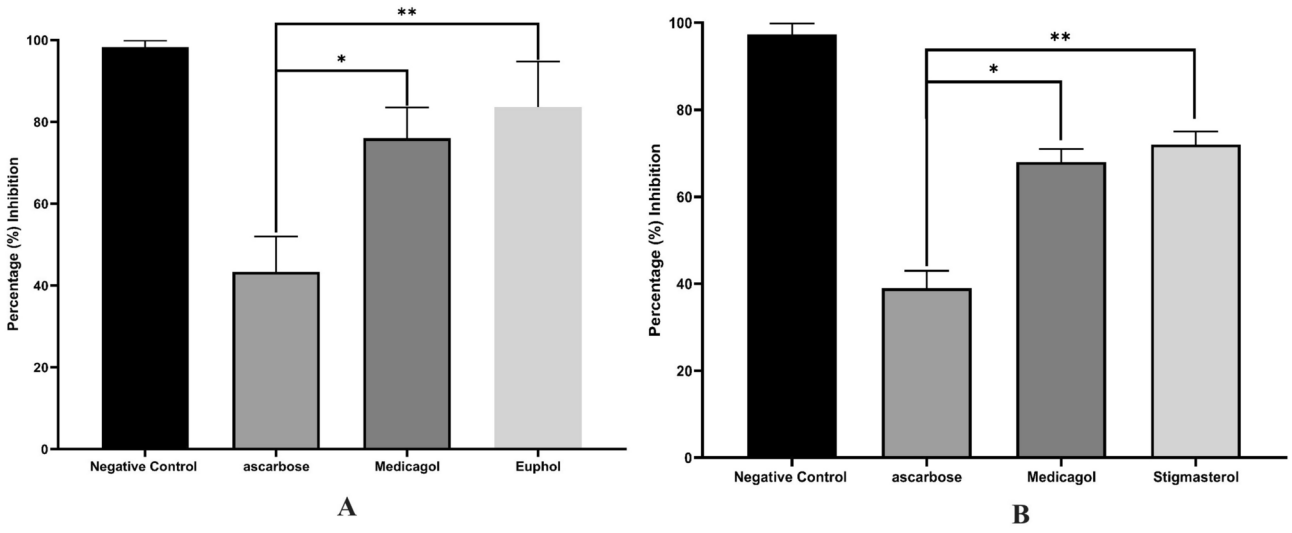

Fig. 8. Percentage inhibition of top-selected phytochemicals against (**A**) alpha-amylase and (**B**) alpha-glucosidase. The experiment was performed in triplicate and the values are shown as mean ± standard error of the mean. If the *p-value* is > 0.05, the results were considered statistically significant, represented by * vs. control. ** *p-value* > 0.01 vs. control was considered very significant.

In vitro inhibitory activity of α-glucosidase

All the phytochemicals were tested against the inhibitory of α-glucosidase. Stigmasterol and Medicagol were more potent inhibitors of α-glucosidase than acarbose (Fig. 8B). These phytochemicals exhibited highly significant results compared to the acarbose with 95% CI, *p* value < 0.01. Our findings suggest that Stigmasterol and Medicagol have significant potential for type 2 diabetes prevention via inhibition of carbohydrates hydrolyzing enzymes.

In vivo anti-diabetic potential of plant extract against STZ-induced diabetic mice

Plant extracts significantly decrease fasting glucose levels in STZ-induced diabetic mice

Throughout the 21-day experimental period, fasting blood glucose levels were monitored to assess the antidiabetic potential. The diabetic control group displayed a highly significant increase in fasting blood glucose levels compared to the normal control group with levels averaging 429 ± 5.33 mg/dl and a 95% CI of -362.0 to -326.7 ($p < 0.0001$). The treatment with *C. arietinum* extract led to a significant reduction in fasting blood glucose from day 0 to 21 when compared to the positive control (374 ± 5.33 mg/dl; 95% CI 2.046 to 37.29; $p = 0.0276$). Similarly, *H. vulgare* extract treatment resulted in a highly significant decrease in fasting blood glucose compared to the positive group (349 ± 5.23 mg/dl; 95% CI 27.71 to 62.95; $p < 0.0001$) (Fig. 9A).

Plant extracts efficacy in oral glucose tolerance enhancement

The glucose tolerance test (GTT) was conducted to assess the glycemic control capabilities of *C. arietinum* and *H. vulgare* extract in STZ-induced diabetic mice. Both extracts demonstrated positive effects on glucose tolerance, with *C. arietinum* showing a favorable response and *H. vulgare* exhibiting the most pronounced improvement in glucose management among the treated groups (Fig. 10).

Plant extracts efficacy in lowering postprandial glucose levels

The *C. arietinum* extract substantially inhibited pancreatic glucosidase activity (80% reduction), which was statistically significant compared to the positive control. However, the extract's effect on intestinal glucosidase activity (68% reduction) was non-significant, indicating that its primary impact is likely concentrated within the pancreatic enzyme systems rather than the intestinal pathway (Fig. 11A). Conversely, *H. vulgare* extract exhibited a highly significant reduction in both pancreatic (68.42%) and intestinal glucosidase (55%) activities (Fig. 11A, B). This dual inhibition profile suggests that *H. vulgare* can comprehensively suppress glucosidase activity across both digestive regions, which may enhance its efficacy in lowering postprandial glucose levels.

Plant extracts elevated G6PD activity

The glucose-6-phosphate dehydrogenase (G6PD) is a key enzyme in the PPP. Which plays a crucial role in proper glucose utilization, providing NADPH for antioxidant defense and biosynthetic processes. A 50% reduction in G6PD activity observed in diabetic mice, relative to controls highlights a significant impairment in glucose metabolism and cellular redox balance as a result of diabetes. Treatment with *C. arietinum* extract for 21 days resulted in a notable recovery of G6PD activity, with a significant increase (95% CI − 2.184 to − 0.4720, $p = 0.0033$) compared to the positive control. The effects of *H. vulgare* extract were even more pronounced with a highly significant elevation in G6PD activity (95% CI − 4.067 to − 2.355, $p < 0.0001$) compared to the positive control (Fig. 12).

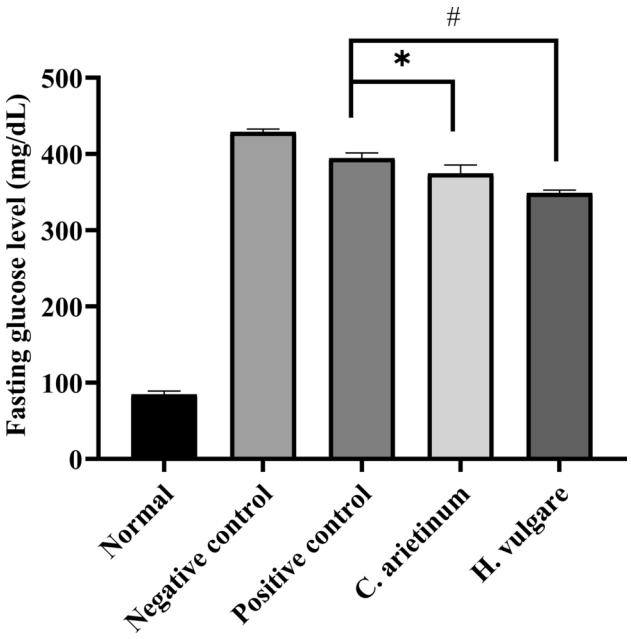

Fig. 9. Effect of *C. arietinum* and *H. vulgare* extracts on fasting blood glucose levels (mg/dl) in streptozotocin (STZ)-induced diabetic mice. Data are presented as mean ± SD (n = 6). Statistical significance is indicated as follows: $p < 0.05$ compared to positive control (*), and $p < 0.0001$ compared to control (#). Statistical analysis was performed using one-way ANOVA followed by Duncan's multiple comparison test.

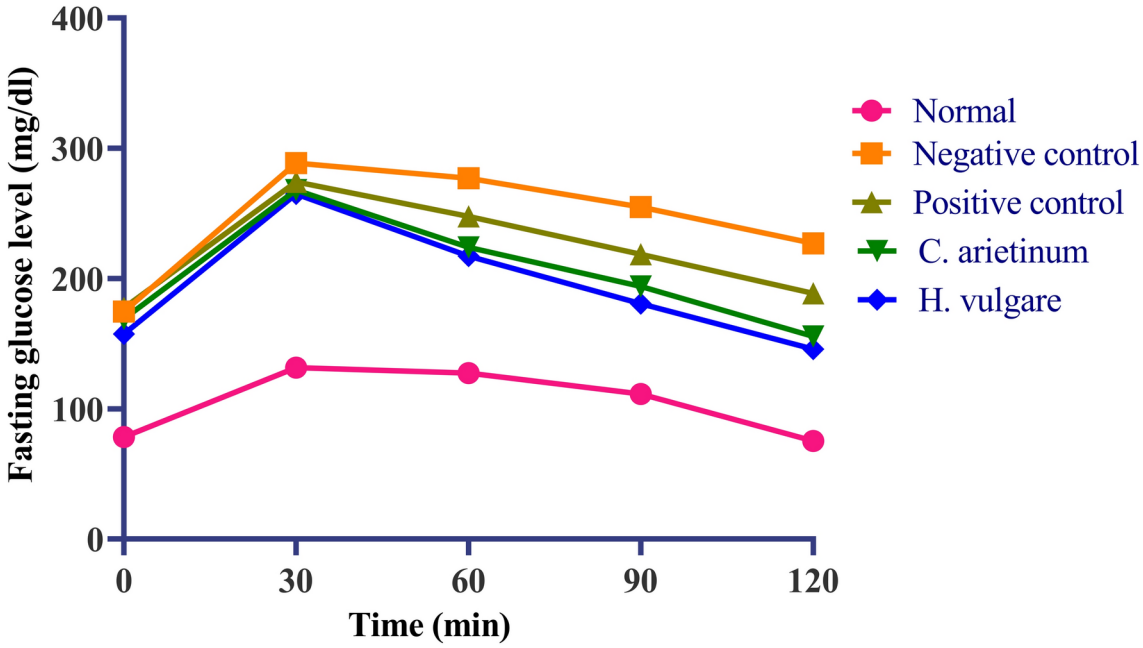

Fig. 10. Oral glucose tolerance after treatment with *C. arietinum* and *H. vulgare* extracts. Data are presented as mean ± SEM (n = 6).

Plant extracts elevated liver and muscle glycogen content

The assessment of hepatic and skeletal muscle glycogen content after treatment with plant extracts in diabetic mice reveals the substantial benefits of these plant extracts in mitigating glycogen depletion caused by diabetes. Diabetic mice exhibited a marked reduction of approximately 45% in glycogen stores in both liver and muscle tissues, underscoring the profound impact of hyperglycemia on glycogen synthesis and storage. Administration of *C. arietinum* extract significantly increased glycogen content in the liver (95% CI −0.3396 to −0.04737, $p = 0.0097$) and muscle (95% CI −0.4504 to −0.03229, $p = 0.0227$), reflecting its potential to restore glycogen

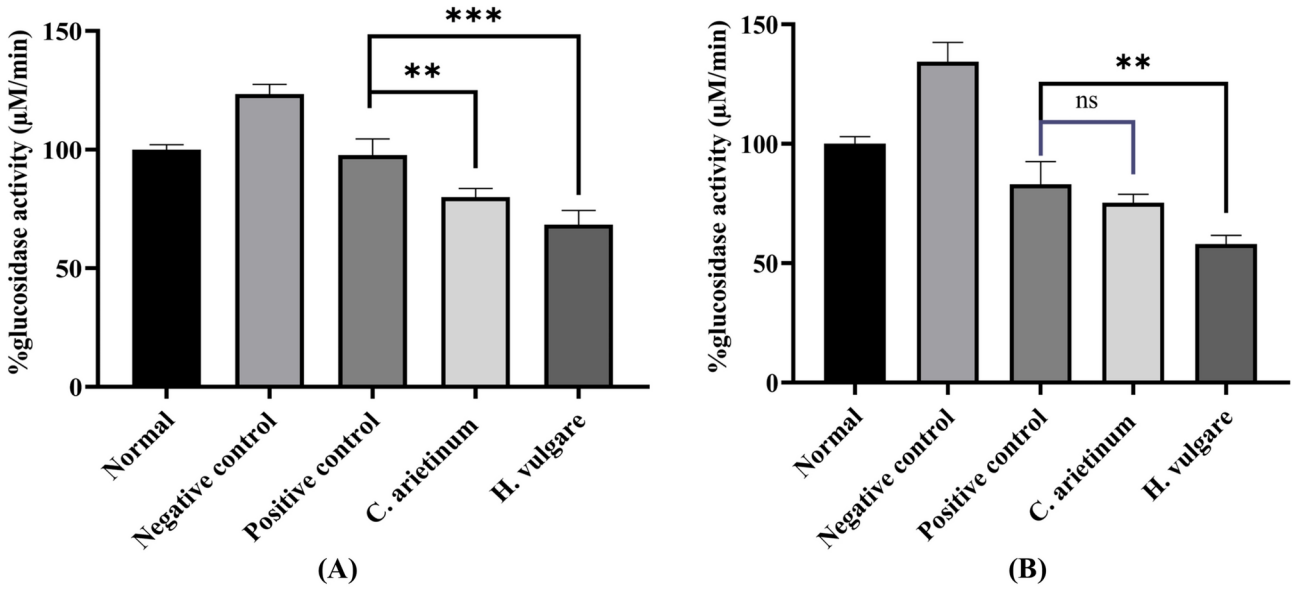

Fig. 11. Post-treatment effects of *C. arietinum* and *H. vulgare* extracts on (**A**) pancreatic and (**B**) intestinal glucosidase activity. Data are presented as Mean ± SEM (n = 6). Statistical significance is denoted as follows; ns ($p > 0.05$) indicates non-significance, $^{**}p < 0.01$, and $^{***}p < 0.001$ compared to control. Statistical analysis was performed using one-way ANOVA followed by Duncan's multiple comparison test.

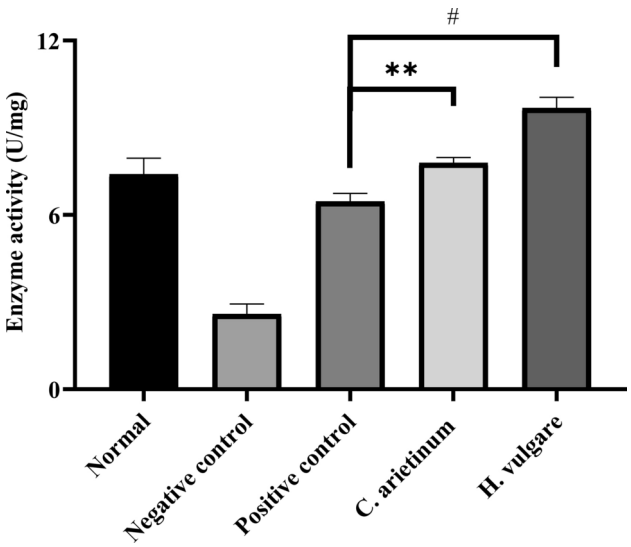

Fig. 12. Restoration of G6PD activity following *C. arietinum* and *H. vulgare* extract treatment. Data are expressed as mean ± SEM (n = 6). Statistical significance is indicated as $p < 0.01$ (**) and $p < 0.0001$ (#) compared to positive control. Analysis was conducted using one-way ANOVA followed by Duncan's multiple comparison test.

stores in diabetic conditions. Similarly, *H. vulgare* extract demonstrated a highly significant improvement in hepatic glycogen levels (95% CI −0.4166 to −0.1244, $p = 0.0009$) and a significant increase in muscle glycogen content (95% CI −0.4794 to −0.06129, $p = 0.0113$) (Fig. 13A, B).

Plant extracts elevated hepatic enzyme in STZ-induced diabetic mice

In diabetic conditions, the serum levels of hepatic enzymes, including ALT, ALP, and AST, and total and direct bilirubin were markedly elevated indicating liver injury and impaired hepatic function associated with diabetes. Treatment with *C. arietinum* extract significantly reduced levels of ALT, ALP, AST, total bilirubin, and direct bilirubin compared to the diabetic control group, suggesting a protective effect of the extract on liver function. The *H. vulgare* extract also showed a highly significant reduction in ALT, AST, ALP, total bilirubin, and direct bilirubin levels exceeding the protective effect observed with other groups (Fig. 14A–E).

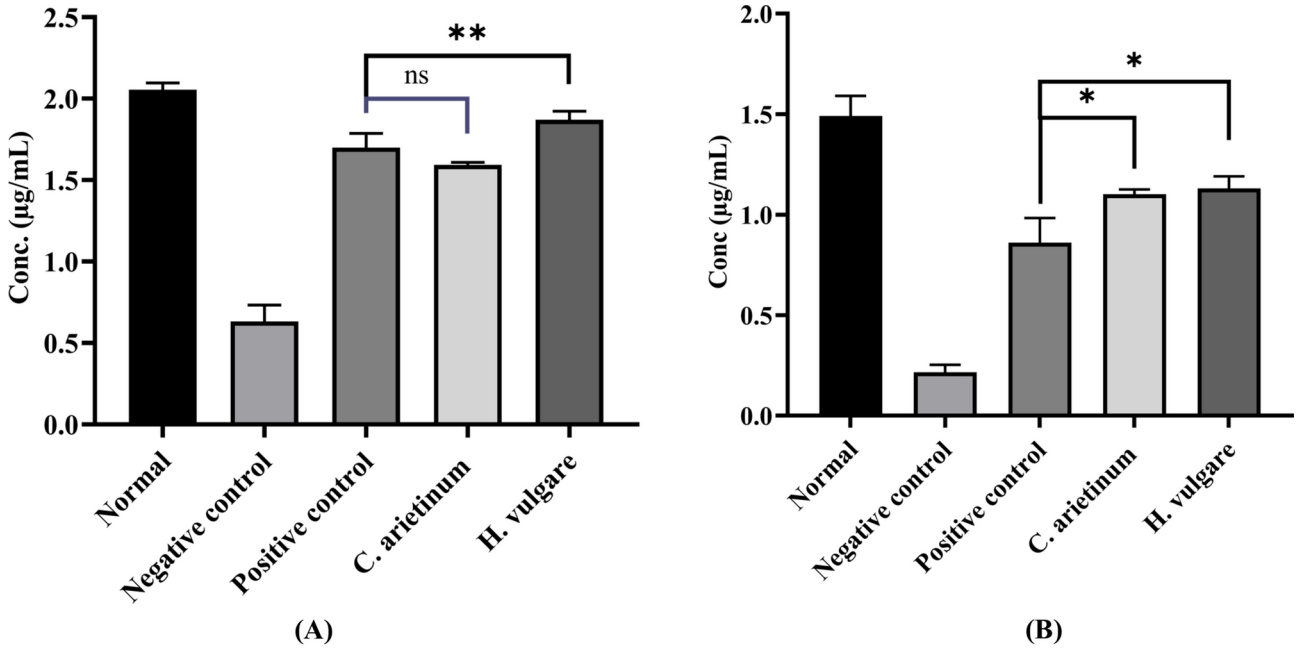

Fig. 13. Glycogen storage in (**A**) liver and (**B**) Skeletal muscle after treatment with *C. arietinum* and *H. vulgare* extracts. Data are presented as mean ± SEM (n = 6). Statistical significance is denoted as $p > 0.05$ (ns), $p < 0.05$ (*), and $P < 0.01$ (**), compared to positive control. Statistical analysis was performed using one-way ANOVA followed by Duncan's multiple comparison test.

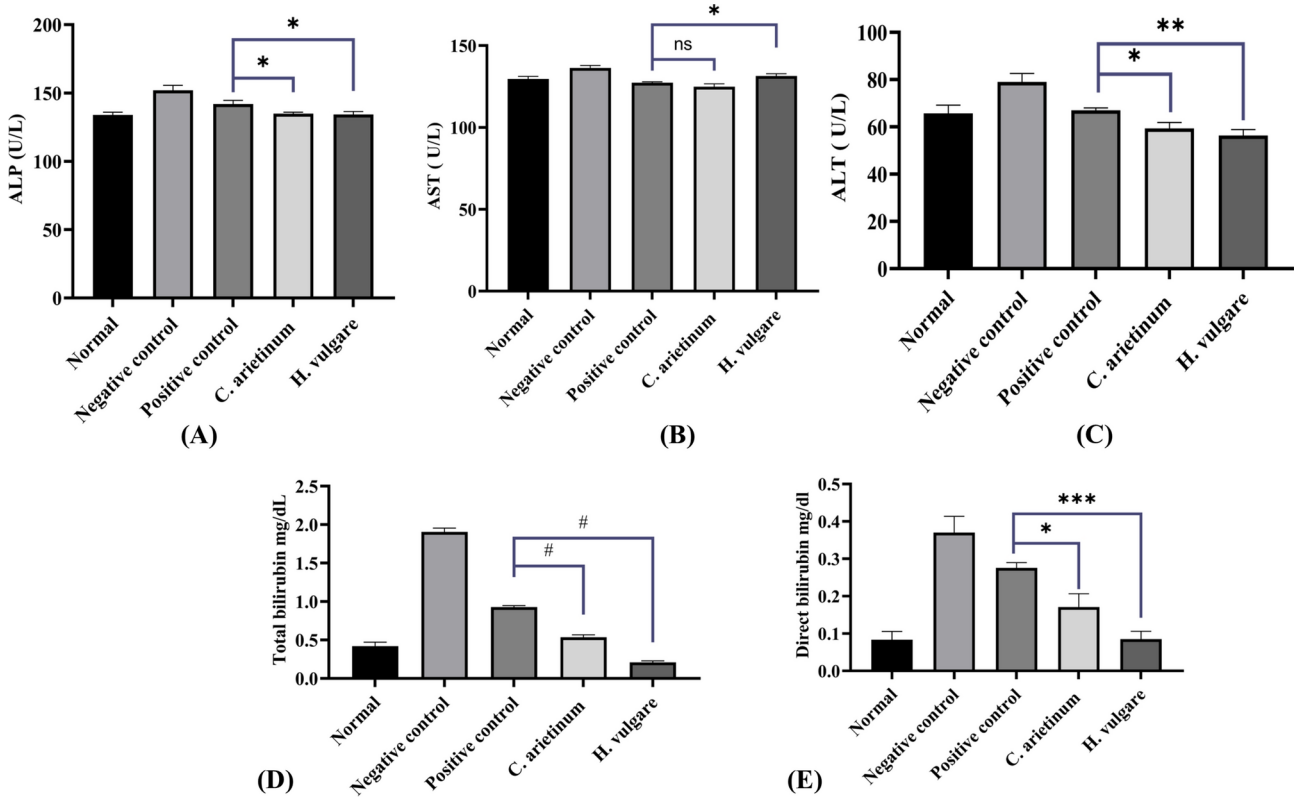

Fig. 14. Effect of *C. arietinum* and *H. vulgare* extracts on liver enzymes in STZ-induced diabetic mice. Shown are (**A**) ALP, (**B**) AST, (**C**) ALT, (**D**) total bilirubin, and (**E**) direct bilirubin levels. Data are expressed as mean ± SEM (n = 6). Statistical significance compared to positive control is indicated as follows: $p > 0.05$ (ns), $P < 0.05$ (*), $P < 0.01$ (**), $P < 0.001$ (***), and $P < 0.0001$ (#). Statistical analysis was performed using one-way ANOVA followed by Duncan's multiple comparison test.

Effect of plant extracts on renal function

In STZ-induced diabetic mice glycosuria, polyuria, and diarrhea were observed from the first week. Treatment with *C. arietinum* extract led to significantly increased plasma urea levels (95% of Cl of difference: 3.429 to 14.22, $p = 0.0012$) and creatinine levels (95% of Cl of difference: 0.09635 to 0.3886, $p = 0.0010$) as compared to the positive control. Additionally, *H. vulgare* extract caused a highly significant elevation in plasma urea (95% of Cl of difference: 3.806 to 14.59, $p = 0.0008$, and creatinine levels (95% of Cl of difference: 0.2975 to 0.5897, $p < 0.001$), indicating a pronounced impact on renal function markers (Fig. 15A, B).

Effect of plant extracts on lipid profile components and serum insulin

STZ-treated mice exhibited significantly elevated cholesterol, triglycerides, LDL, and VLDL levels and reduced HDL levels compared to normal controls. Treatment with *C. arietinum* extract significantly normalized these lipid levels toward those of the positive control (95% of CI $p < 0.0001$, $p < 0.0001$, $p = 0.003$, $p < 0.0001$, and $p < 0.001$ respectively) relative to STZ-induced diabetic mice. In contrast, *H. vulgare* extract treatment led to a highly significant increase in TC, TG, LDL, and VLDL levels with a corresponding decrease in HDL as compared to the positive control, indicating an adverse effect on lipid profile parameters (Fig. 16A–E).

Serum insulin levels were markedly reduced in the STZ-induced diabetic mice model as compared to the non-diabetic control group, reflecting the characteristic beta-cell destruction and consequent insulin deficiency associated with STZ-induced diabetes. In contrast, the *C. arietinum* extract showed a significant increase in serum levels (95% of CI −33.50 to −8.670, $p = 0.0008$) as compared to the positive control group. Conversely, treatment with *H. vulgare* extract showed highly significant serum insulin levels (95% of CI −38.59 to −13.67, $p < 0.001$) as compared to the positive control, suggesting a potential protective or restorative effect on pancreatic function or insulin secretion (Fig. 16F). This improvement aligns with the extract's observed lipid-lowering effect. Which could further contribute to an improved metabolic profile in diabetic conditions.

Effect of plant extracts on oxidative stress

The antioxidant profile, including superoxide dismutase (SOD), catalase (CAT), glutathione (GSH), and malondialdehyde (MDA) was evaluated in liver, kidney, and pancreas tissues of STZ-diabetic mice with C. arietinum and H. vulgare extracts in comparison to normal, negative control, positive control groups.

Oxidative stress markers of liver In *C. arietinum* extract-treated mice, the SOD activity in liver tissue showed no significant difference compared to the positive controls (95% of CI −0.5143 to 10.51; $p = 0.0847$). However, *H. vulgare* extract treatment resulted in a highly significant increase in SOD activity (95% of CI 5.836 to 16.86; $p = 0.001$). The activity of CAT was significantly enhanced in both extracts treated groups. In the *C. arietinum* group, CAT activity increased significantly (95% of CI −13.88 to −2.123; $p = 0.0059$), while *H. vulgare* led to a very highly significant increase in CAT activity (95% of CI −21.88 to −10.12; $p < 0.0001$) compared to the positive control. The levels of GSH in the *C. arietinum* group did not show significant improvement (95% CI −6.471 to 1.006; $p = 0.2124$), suggesting a limited effect on enhancing endogenous antioxidant reserves in this group. However, *H. vulgare* extract treatment significantly elevated GSH levels (95% CI −8.064 to −0.5862; $p = 0.0199$). Both extracts significantly reduced MDA concentrations in liver tissue compared to the positive control, with *C.*

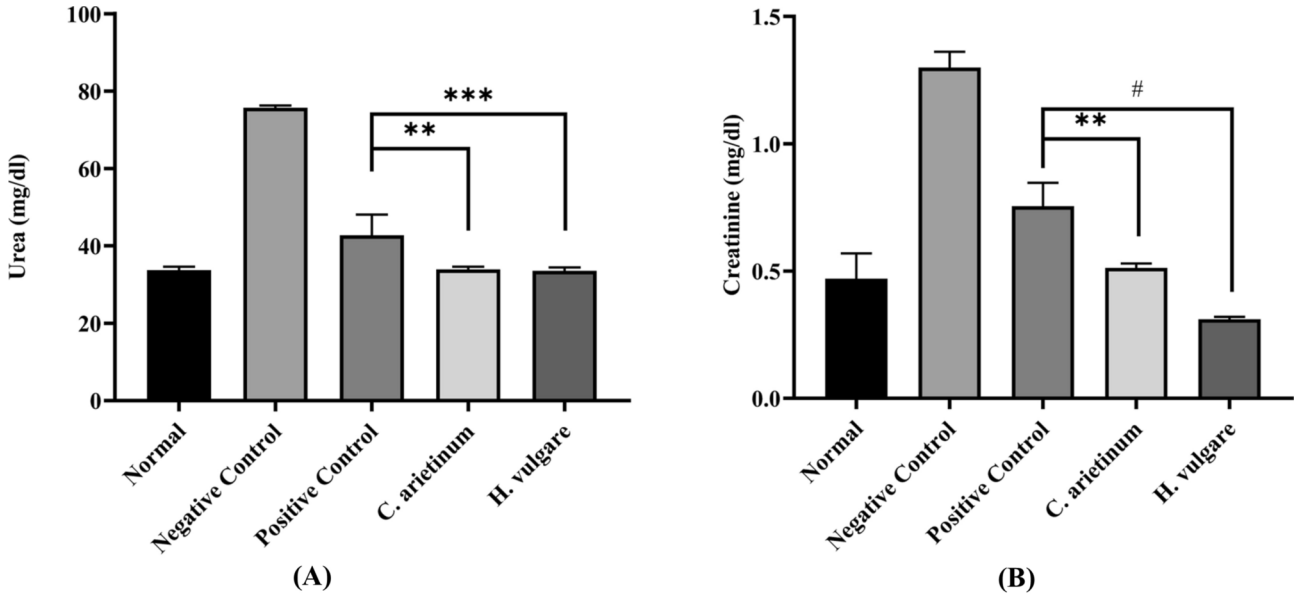

Fig. 15. Impact of *C. arietinum* and *H. vulgare* extracts on renal function markers in STZ-induced diabetic mice. Shown are levels of (**A**) Urea and (**B**) Creatinine. Data are presented as mean ± SEM (n = 6). Statistical significance compared to positive control is indicated by $p < 0.01$ (**), $P < 0.001$ (***), and $P < 0.0001$ (#). Statistical analysis was conducted one-way ANOVA followed by Duncans multiple comparison test.

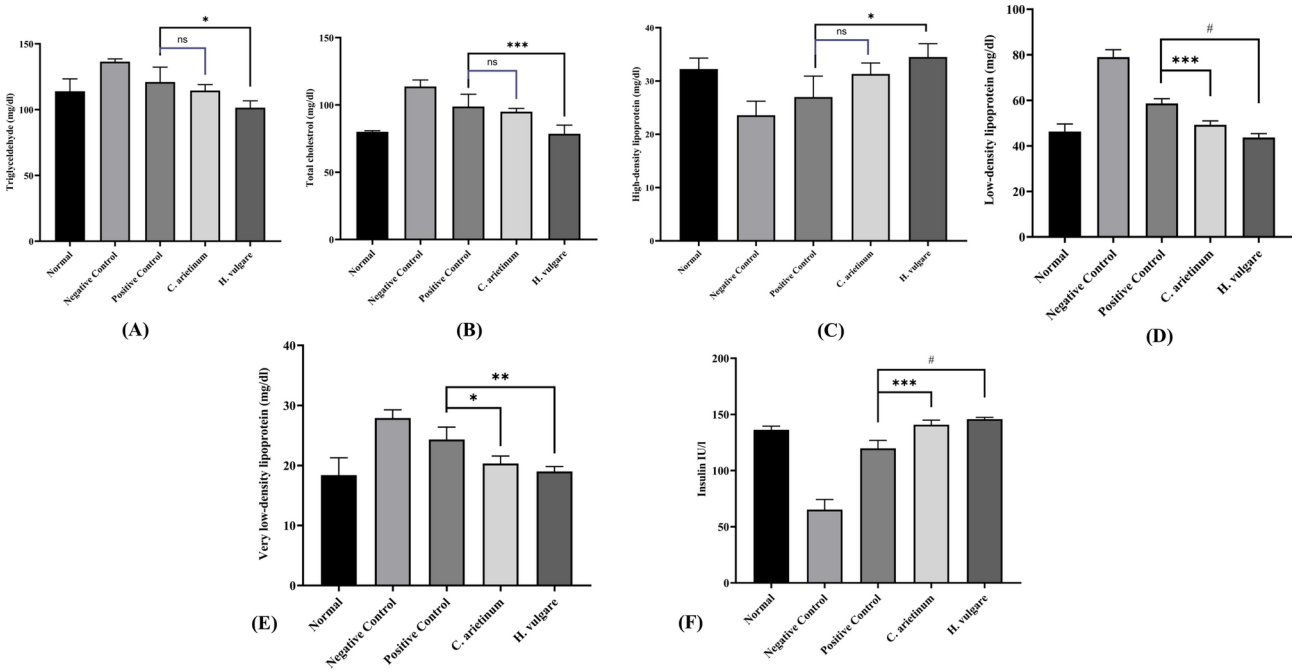

Fig. 16. Effect of *C. arietinum* and *H. vulgare* extracts on lipid profile and insulin levels in STZ-induced diabetic mice. Parameters assessed include (**A**) triglycerides, (**B**) total cholesterol, (**C**) high-density lipoprotein (HDL), (**D**) low-density lipoprotein (LDL), (**E**) very low-density lipoprotein (VLDL), and (**F**) insulin levels. Data are expressed by mean ± SEM (n = 6). Statistical significance compared to positive control is indicated as follows; $p > 0.05$ (ns), $p < 0.05$ (*), $p < 0.01$ (**), $p < 0.001$ (***), and $p < 0.0001$ (#). Statistical analysis was conducted using one-way ANOVA followed by Duncan's multiple comparison test.

arietinum (95% CI 0.02967 to 0.5063, $p = 0.0241$) and *H. vulgare* (95% CI 0.04942–0.5261, $p = 0.0147$) treatments achieving a noteworthy reduction (Fig. 17A–D).

Oxidative stress markers of kidney For superoxide dismutase (SOD) activity in kidney tissue, *C. arietinum* extract administration showed a nonsignificant change (95% CI, −0.3750 to 5.945, $p = 0.0947$) compared to the positive control. However, *H. vulgare* extract significantly increased SOD activity (95% CI 1.290 to 7.610, $p = 0.0044$) compared to the positive control. Regarding catalase (CAT) activity, *C. arietinum* extract also showed a nonsignificant effect (95% CI −10.96 to 2.616, $p = 0.3596$). Conversely, *H. vulgare* extract exhibited a highly significant increase in CAT activity (95% CI −15.60 to −2.021, $p = 0.0086$), suggesting that it effectively reduces hydrogen peroxide accumulation. For glutathione (GSH) levels, *C. arietinum* extract did not significantly alter GSH concentration (95% CI −3.973 to 5.223, $p = 0.9928$). However, *H. vulgare* significantly increased GSH levels (95% CI −10.35 to −1.152, $p = 0.0114$) as compared to the positive control, indicating an enhancement of glutathione reserve and potentially improved detoxification capacity within renal cells. Lipid peroxidation as indicated by MDA levels showed significant changes with *C. arietinum*, 95% CI 0.01597 to 0.6710, $p = 0.0377$. while *H. vulgare* extract showed high significance with 95% CI 0.2640 to 0.9190, $p = 0.0004$ suggesting that treatment has a substantial effect on lipid oxidation in the kidney under these experimental conditions (Fig. 18A–D).

Oxidative stress markers of the pancreas The activity of superoxide dismutase (SOD) in pancreatic tissue was significantly elevated in both *C. arietinum* and *H. vulgare* extract-treated groups compared to the positive control. The C. arietinum group demonstrated a notable increase in SOD activity (95% CI −5.502 to −1.538, $p = 0.0012$). Similarly, *H. vulgare* exhibited a highly significant effect on SOD levels (95% CI −6.626 to −2.661, $p = 0.0001$). Catalase (CAT) activity essential for detoxifying hydrogen peroxide in pancreatic tissue, displayed a significant response to *C. arietinum* treatment (95% CI −4.441 to −0.2456, $p = 0.0275$). However, *H. vulgare* extract highly significantly boosted CAT activity (95% CI −6.801 to −2.606, $p = 0.0002$) compared to the positive control, indicating a more robust effect on enhancing pancreatic antioxidant defenses. Regarding GSH levels, both extracts effectively raised GSH concentrations, with *C. arietinum* showing a highly significant increase (95% CI −3.084 to −1.083, $p = 0.0003$) and *H. vulgare* demonstrating a highly significant elevation (95% CI −4.950 to −2.950, $p < 0.0001$) as compared to the positive control. The *C. arietinum* group highly significantly lowered MDA levels (95% CI −1.320 to −0.5246, $p = 0.0001$), while *H. vulgare* showed an even greater reduction with high significance (95% CI −2.180 to −1.385, $p < 0.0001$) as compared to the positive control, indicating that both extracts mitigate lipid peroxidation, helping preserve cellular membrane integrity in pancreatic cells under oxidative stress (Fig. 19A–D).

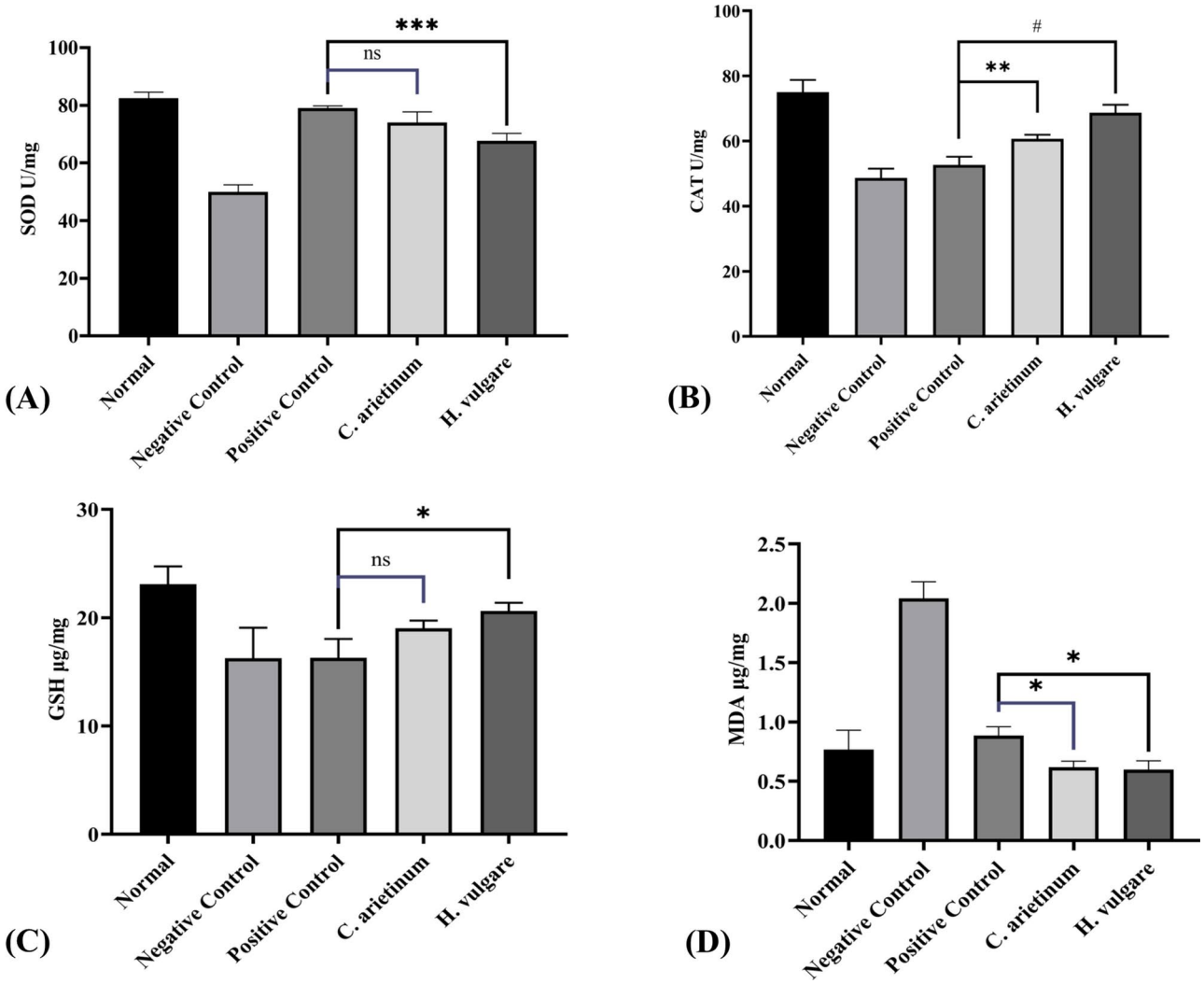

Fig. 17. Effect of *C. arietinum* and *H. vulgare* extracts on hepatic oxidative stress biomarkers in STZ-induced diabetic mice. The biomarkers evaluated include (**A**) superoxide dismutase (SOD), (**B**) catalase (CAT), (**C**) reduced glutathione (GSH), and (**D**) malondialdehyde (MDA). Data are presented as mean ± SEM (n = 6). Statistical significance compared to positive control is denoted as follows: $p > 0.05$ (ns), $p < 0.05$ (*), $p < 0.01$ (**), $p < 0.001$ (***), and $p < 0.0001$ (#). Statistical analysis was performed using one-way ANOVA followed by Duncan's multiple comparison test.

Histopathological examination of STZ-induced diabetic mice

The histological analysis of pancreatic and liver tissues provides valuable insights into the protective effects of *C. arietinum* and *H. vulgare* on pancreatic and liver integrity under diabetic conditions.

Histopathological lesions in the pancreas The Normal control group mice displayed a healthy pancreatic structure with intact exocrine and endocrine regions (Fig. 20A), establishing a baseline of morphological normalcy. In contrast, negative control group mice exhibited normal exocrine morphology but showed a reduction in the number and mass of islet cells in the endocrine pancreas (Fig. 20B). Similarly, while showing a structurally intact exocrine pancreas, the positive control mice presented a reduction in islet cell mass (Fig. 20C), which reflects ongoing degenerative changes in the endocrine pancreas due to hyperglycemic stress. Notably, the *C. arietinum* extract-treated group revealed normal exocrine morphology but notable degenerative changes in the endocrine pancreas, leading to diminished islet cell size and quantity (Fig. 20D). The protective potential of *H. vulgare* extract group treatment became more pronounced, which displayed normal morphology in both exocrine and endocrine pancreatic regions (Fig. 20E), indicating a stimulating effect on islet cells and suggesting effective mitigation of diabetes-induced damage.

Histopathological lesions in the liver The normal control group displayed preserved liver morphology, characterized by well-defined hepatic lobules, intact cellular architecture, and structurally sound hepatocytes (Fig. 21A). Conversely, the negative control group demonstrated clear signs of liver injury, likely due to the hyperglycemia-associated oxidative stress. Liver sections from this group exhibited pronounced histological

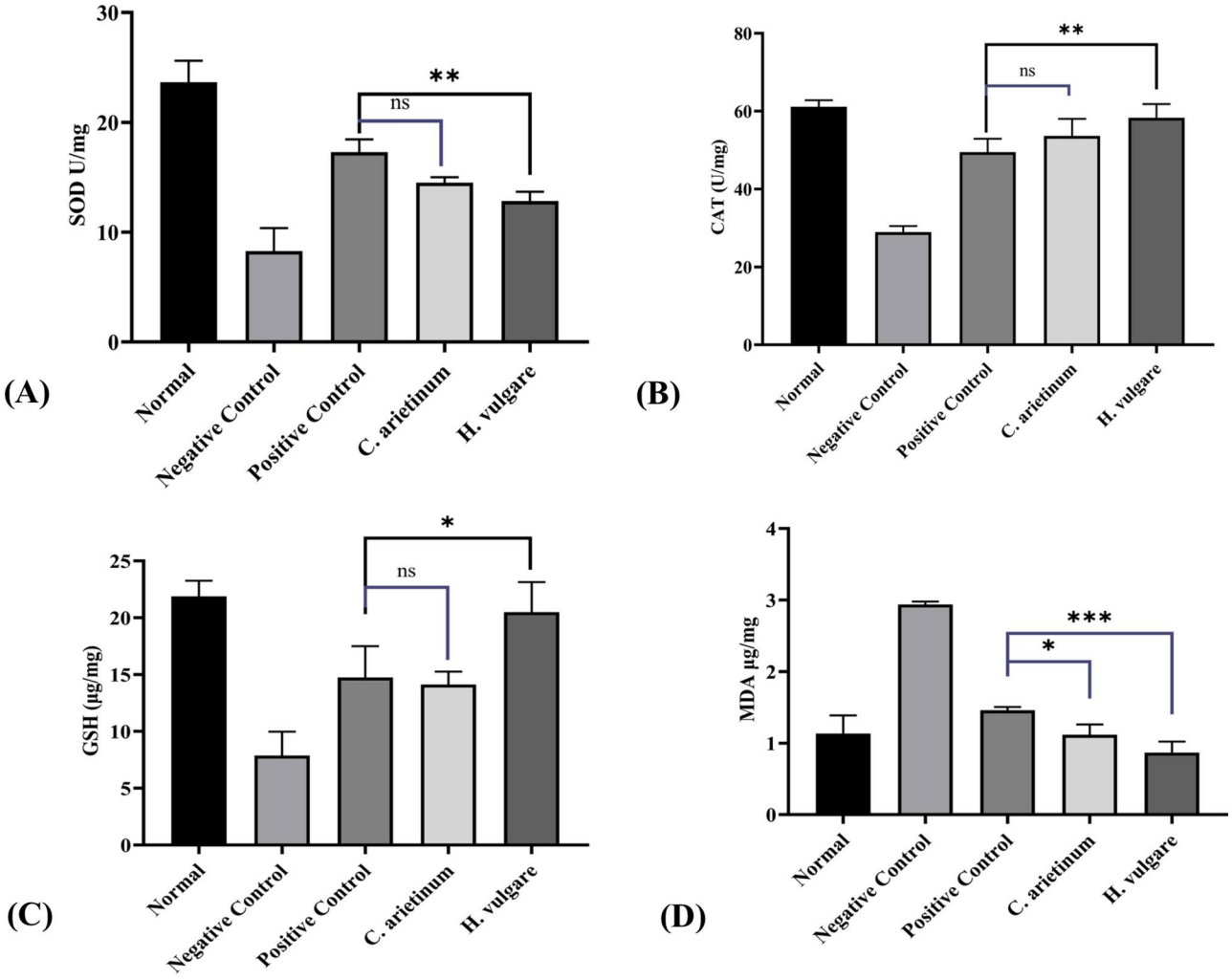

Fig. 18. Effect of *C. arietinum* and *H. vulgare* extracts on Renal Oxidative Stress Biomarkers in STZ-induced Diabetic Mice. The biomarkers evaluated include (**A**) superoxide dismutase (SOD), (**B**) catalase (CAT), (**C**) reduced glutathione (GSH), and (**D**) malondialdehyde (MDA). Data are presented as mean ± SEM (n = 6). Statistical significance compared to positive control is denoted as follows: $p > 0.05$ (ns), $p < 0.05$ (*), $p < 0.01$ (**), and $p < 0.001$ (***). Statistical analysis was performed using one-way ANOVA followed by Duncan's multiple comparison test.

alterations, including hepatocyte degeneration, reduced cell mass, and architectural distortions, indicative of significant hepatic damage (Fig. 21B). Similar pathological features were observed in the positive control group, such as hepatocyte loss and structural disruptions, underscoring the detrimental impact of diabetes on liver integrity (Fig. 21C). The *C. arietinum* extract-treated group showed partial preservation of hepatic architecture, with moderate hepatocyte degeneration still visible, suggesting an initial protective effect against diabetes-induced liver damage (Fig. 21D). In the *H. vulgare* treated group, histological examination revealed near complete restoration of liver morphology, with structurally intact hepatocytes and minimal to no observable degenerative changes (Fig. 21E).

Discussion

The obesity epidemic and type 2 diabetes mellitus (T2DM) are both serious global health problems. People with T2DM are at substantial risk for both micro-vascular issues because of hyperglycemia and specific components of the insulin resistance (metabolic) syndrome[65,66]. It is important to note that the experimental setup primarily involved an STZ-induced diabetic mouse model, which may not fully replicate the complexity of human diabetes. Factors such as genetic variability, environmental influences, and dietary habits in humans could alter the efficacy and safety of these extracts. Additionally, the concentrations of phytochemicals used in this study may not directly translate to achievable levels in clinical scenarios emphasizing the need for dose optimization studies in humans. This study employed multiple experimental approaches, including in silico modeling, in vivo analysis, and biochemical assays. While this multifaceted approach strengthens the overall findings, it introduces complexity in interpretation. To address this, we compared and integrated results across these methodologies. For instance, in silico docking identified key phytochemicals with strong binding affinities to diabetes related

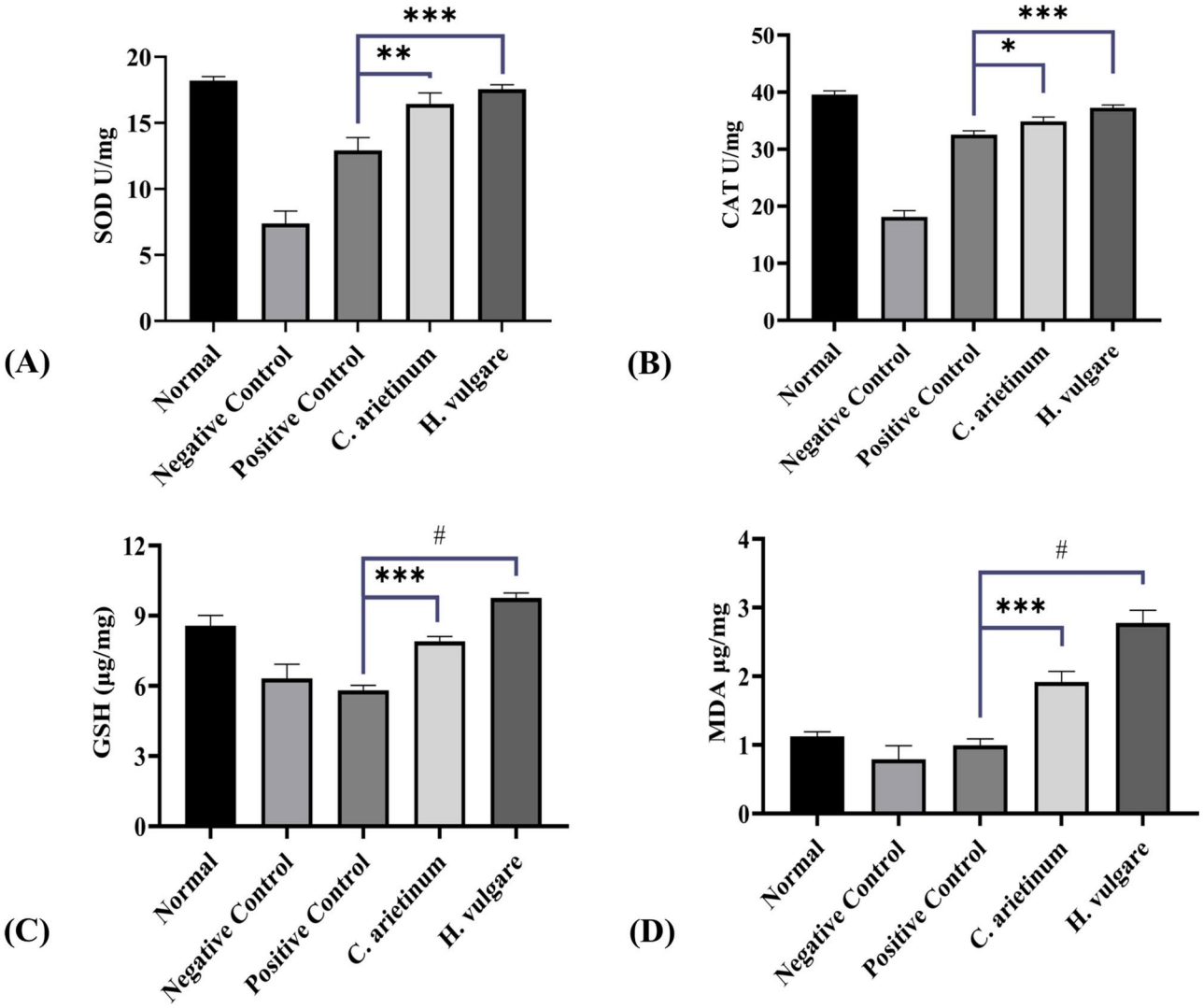

Fig. 19. Effect of *C. arietinum* and *H. vulgare* Extracts on Pancreatic Oxidative Stress Biomarkers in STZ-induced Diabetic Mice. The biomarkers evaluated include (**A**) superoxide dismutase (SOD), (**B**) catalase (CAT), (**C**) reduced glutathione (GSH), and (**D**) malondialdehyde (MDA). Data are presented as mean ± SEM (n = 6). Statistical significance compared to positive control is denoted as follows: $p < 0.05$ (*), $p < 0.01$ (**), and $p < 0.001$ (***). Statistical analysis was performed using one-way ANOVA followed by Duncan's multiple comparison test.

targets. These were corroborated by the in vivo results, which demonstrated significant improvement in glucose tolerance and insulin sensitivity thus validating the computational predictions. However, some discrepancies were observed such as the weak in vivo activity of certain phytochemicals predicted to be potent inhibitors likely due to bioavailability or metabolic factors. Our in-silico findings demonstrated that Medicagol emerged as the most promising drug candidate with no violations of Lipinski's rules, the best docking score, and strong amino acid interactions at the active site of the target receptor. Medicagol also exhibited favorable ADMET (absorption, distribution, metabolism, excretion, and toxicity), showing non-toxic and non-carcinogenic behavior. The second-best phytochemicals Euphol and stigmasterol, violated only one rule and were not identified as AMES toxins making them additional potential candidates for diabetes treatment. in contrast, the remaining phytochemicals were found to violate multiple rules and displayed toxic and carcinogenic properties, rendering them unsuitable as drug candidates. These results emphasize the critical role of ADMET properties in drug development, as they directly impact therapeutic agents' pharmacokinetics, safety, and efficacy.

The molecular docking and MD simulations provided insights into the binding affinities and dynamic behavior of the protein–ligand complexes[67]. Medicagol demonstrated stable binding within the receptor site during the 100 ns simulations, as evidenced by minimal deviations in RMSD values and well-maintained hydrogen bond interactions. RMSF analysis further identified protein regions with higher flexibility, indicating their potential role in ligand binding and enzyme activity. Previous studies by Zhang et al.[68] reinforce the importance of docking simulations for identifying promising bioactive compounds. phytochemicals such as Medicagol, Guanidines, Flemichin D, and Naringenin exhibited strong binding affinities to diabetes related targets, highlighting their

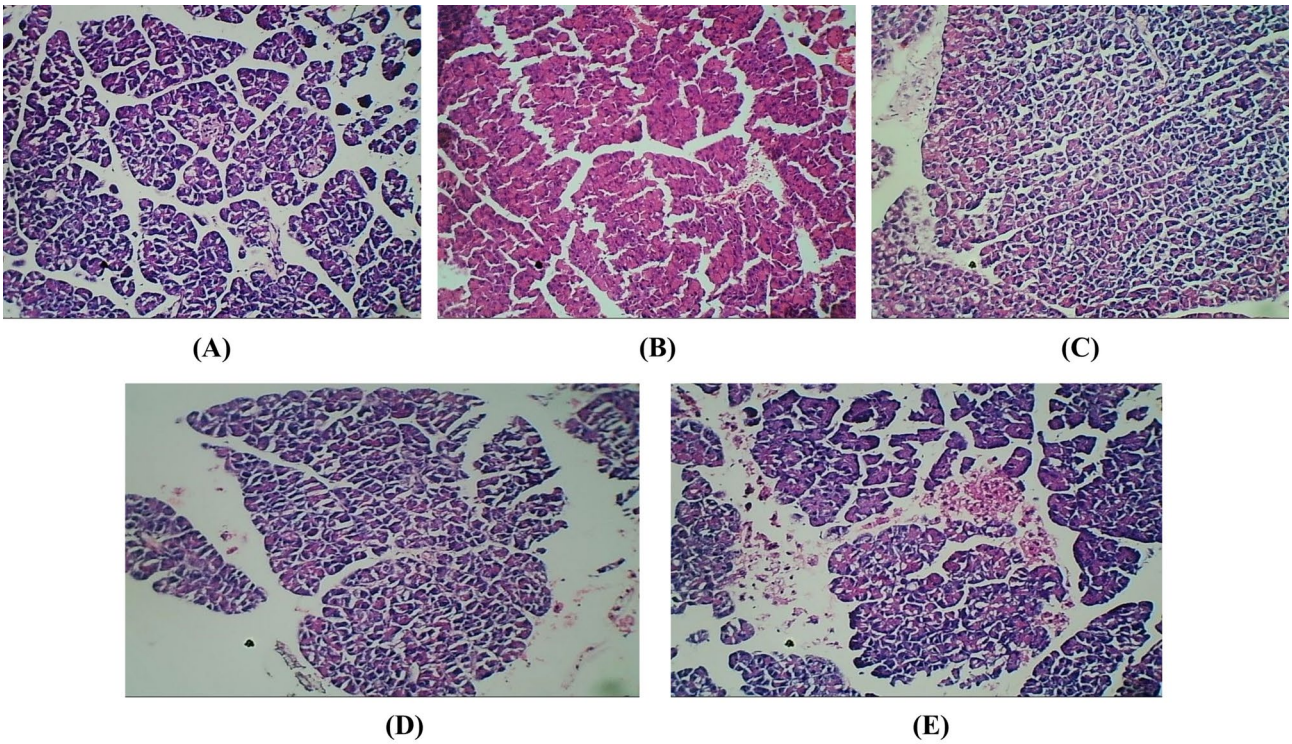

Fig. 20. Histological analysis of pancreas following *C. arietinum* and *H. vulgare* extract treatments in STZ-induced diabetic mice (100× magnification). (**A**) normal control group showing typical pancreatic architecture, (**B**) Negative control (diabetic) group displaying altered morphology, (**C**) Positive control treated with acarbose exhibiting improved pancreatic structure, (**D**) *C. arietinum* extract treatment (5.5 mg/g) showing restoration of normal pancreatic morphology, (**E**) *H. vulgare* extract treatment (11.6 mg/g) indicating histological improvement.

potential in alleviating diabetic symptoms through antioxidative, methylglyoxal trapping, and anti-inflammatory mechanisms. These studies underscore the efficacy of computational approaches in advancing antidiabetic drug discovery.

The in vivo experiments demonstrated the antihyperglycemic effects of *C. arietinum* (chickpea) and *H. vulgare* (barley) extracts in STZ-induced diabetic mice. STZ administration induced hyperglycemia by selectively destroying pancreatic β-cells providing a reliable model for evaluating the therapeutic efficacy of plant extracts[69]. Treatment with these extracts significantly reduced fasting blood glucose levels particularly by day 10, with maximal therapeutic effects observed by day 15[69]. This antihyperglycemic activity can be attributed to their ability to inhibit α-glucosidase enzymes in the pancreas and small intestine thereby reducing postprandial hyperglycemia (PPHG) by delaying carbohydrate digestion and glucose absorption[69]. A 50% decrease in glucosidase activity in vivo was observed further supporting their potential to modulate glycemic control effectively.

The study also highlighted the role of the pentose phosphate pathway (PPP) in glucose metabolism, specifically through glucose-6-phosphate dehydrogenase (G6PD)[70–72]. STZ-induced diabetes significantly reduced G6PD activity, impairing glucose utilization and exacerbating oxidative stress. Treatment with *C. arietinum* and *H. vulgare* extracts resorted hepatic G6PD activity, facilitating NADPH production which is essential for oxidative stress defense and normal cellular functions. This restoration may be linked to insulin regulation as G6PD activity is closely correlated with insulin levels. By enhancing PPP activity, these extracts further demonstrated their antihyperglycemic properties[73].

Insulin also plays a critical role in glycogen synthesis, and diabetes-induced insulin deficiency disrupts glycogen storage in the liver and skeletal muscle (Fig. 22)[74–76]. This study observed a significant reduction (50%) in glycogen content in diabetic mice, which was markedly reversed upon treatment with *C. arietinum* and *H. vulgare* extracts. This effect was likely mediated by reactivation of glycogen synthase thereby restoring glycogen storage and mitigating muscle wasting associated with diabetes.

Liver enzyme activity and bilirubin levels key biomarkers of hepatic damage were significantly elevated in untreated diabetic mice due to oxidative stress and inflammation[77–80]. Treatment with *C. arietinum* and *H. vulgare* extracts significantly reduced ALT, ALP, AST, and bilirubin levels demonstrating a protective effect on liver function. This hepatoprotective response is attributed to phytoconstituents such as tannins, flavonoids, rutin, and phenolic glycosides which possess potent antioxidant and anti-inflammatory properties[81–83]. These compounds likely mitigate reactive oxygen species (ROS) production thereby protecting hepatic cells from oxidative stress and inflammation.

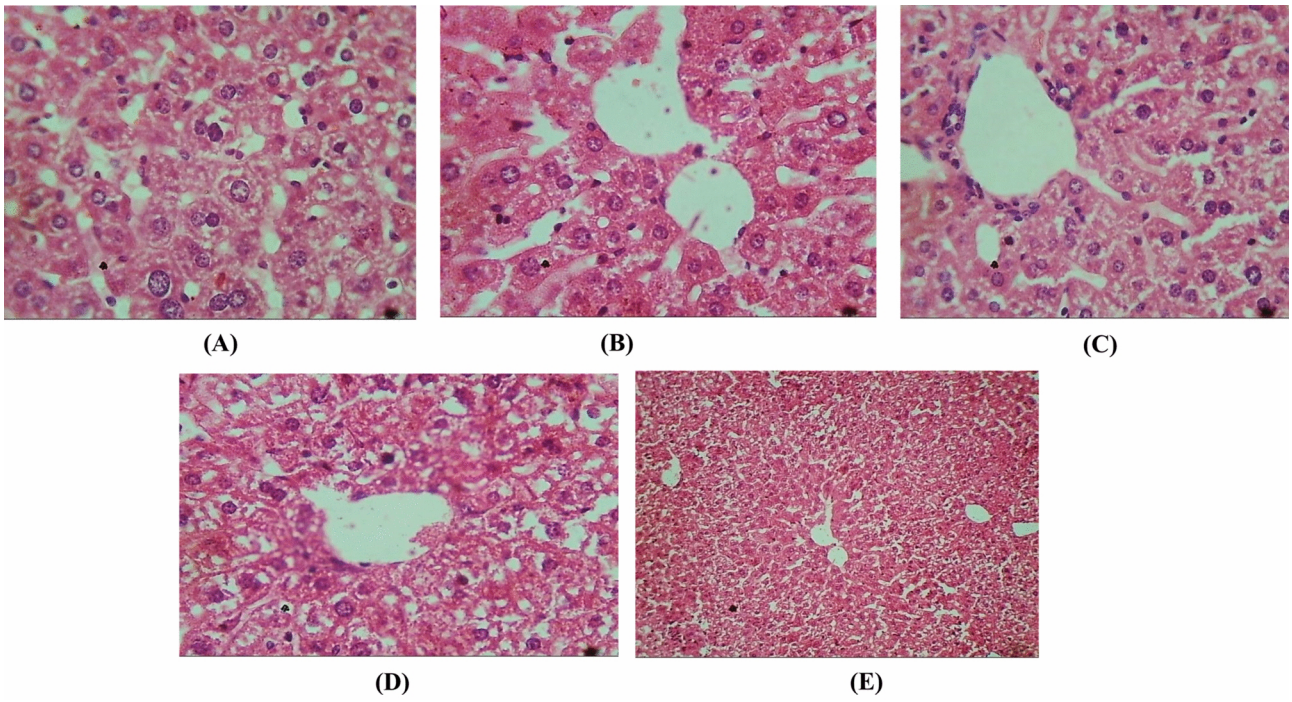

Fig. 21. Histological analysis of liver following *C. arietinum* and *H. vulgare* extract treatments in STZ-induced diabetic mice (40× magnification). (**A**) Normal control group showing typical liver morphology, (**B**) Negative Control (Diabetic) group with altered liver structure, (**C**) Positive control treated with acarbose showing improved liver architecture, (**D**) *C. arietinum* extract treatment (5.5 mg/g) demonstrating restoration of normal liver morphology, (**E**) *H. vulgare* extract treatment (11.6 mg/g) indicating histological improvement.

Similarly, renal function biomarkers (Urea and Creatinine) indicated significantly renal damage in diabetic mice, a common complication of diabetes[84–86]. Elevated levels of these markers were reduced following treatment with the plant extracts suggesting improved kidney function. The phytoconstituents likely counteracted oxidative stress and inflammation within renal tissues, enhancing glomerular filtration and renal health.

Dyslipidemia another hallmark of diabetes is characterized by elevated triglycerides and disrupted lipid metabolism due to insulin deficiency[87,88]. Our study demonstrated significant improvements in the lipid profile of diabetic mice treated with *C. arietinum* and *H. vulgare* extracts. Polyphenolic compounds in these extracts likely exerted lipid-lowering effects by modulating lipid absorption, enhancing lipid metabolism, and reducing oxidative stress[89–92]. These findings align with previous reports highlighting the role of polyphenols in improving lipid profiles and preventing lipid peroxidation in diabetic conditions.

Oxidative stress plays a central role in the pathogenesis of diabetes by exacerbating hyperglycemia, hyperlipidemia, and cellular dysfunction in key metabolic tissues such as the kidney, liver, and pancreas[93,94]. Elevated ROS levels impair insulin secretion and signaling, worsening metabolic dysfunction and accelerating diabetic complications[95,96]. The antioxidant properties of *C. arietinum* and *H. vulgare* mediated by their bioactive phytoconstituents were evident in their ability to mitigate ROS production and enhance cellular antioxidant defense mechanisms[97–99].

The histopathological analysis of the liver and pancreas in diabetic mice treated with *C. arietinum* and *H. vulgare* extracts revealed significant tissue protection and regeneration likely mediated by the antioxidant and anti-inflammatory properties of the plant's phytochemicals. Phytochemicals particularly polyphenols, flavonoids, tannins, and amino acids have been widely recognized for their potential to mitigate oxidative stress, reduce inflammation, and promote tissue regeneration which are critical for counteracting the damage induced by diabetes[100,101]. In the pancreas, histopathological examination showed significant protection and potential regeneration of pancreatic β-cells[101]. This diabetic control mice exhibited severe structural degenerative changes. In contrast, treatment with *C. arietinum* and *H. vulgare* extracts led to notable preservation of pancreatic tissue, restoring the number and morphology of islet cells. This regenerative effect may be attributed to tannins and flavonoids, which have been shown to exert anti-inflammatory effects and promote the proliferation of progenitor cells involved in β-cell regeneration[101,102].

Additionally, the observed antioxidant activity of *C. arietinum* and *H. vulgare* extracts likely contributed to reducing oxidative stress in the pancreas further supporting tissue recovery. In the liver, diabetic mice showed signs of hepatocellular injury with increased inflammation, hepatocyte degeneration, and disrupted hepatic architecture[103]. Treatment with *C. arietinum* and *H. vulgare* extracts resulted in substantial improvement in liver morphology, including a reduction in inflammatory cell infiltration and the restoration of normal hepatic architecture. This effect may be attributed to the plant's polyphenolic compounds, which possess potent antioxidant properties that protect against lipid peroxidation and oxidative damage[104]. Moreover, the tannins

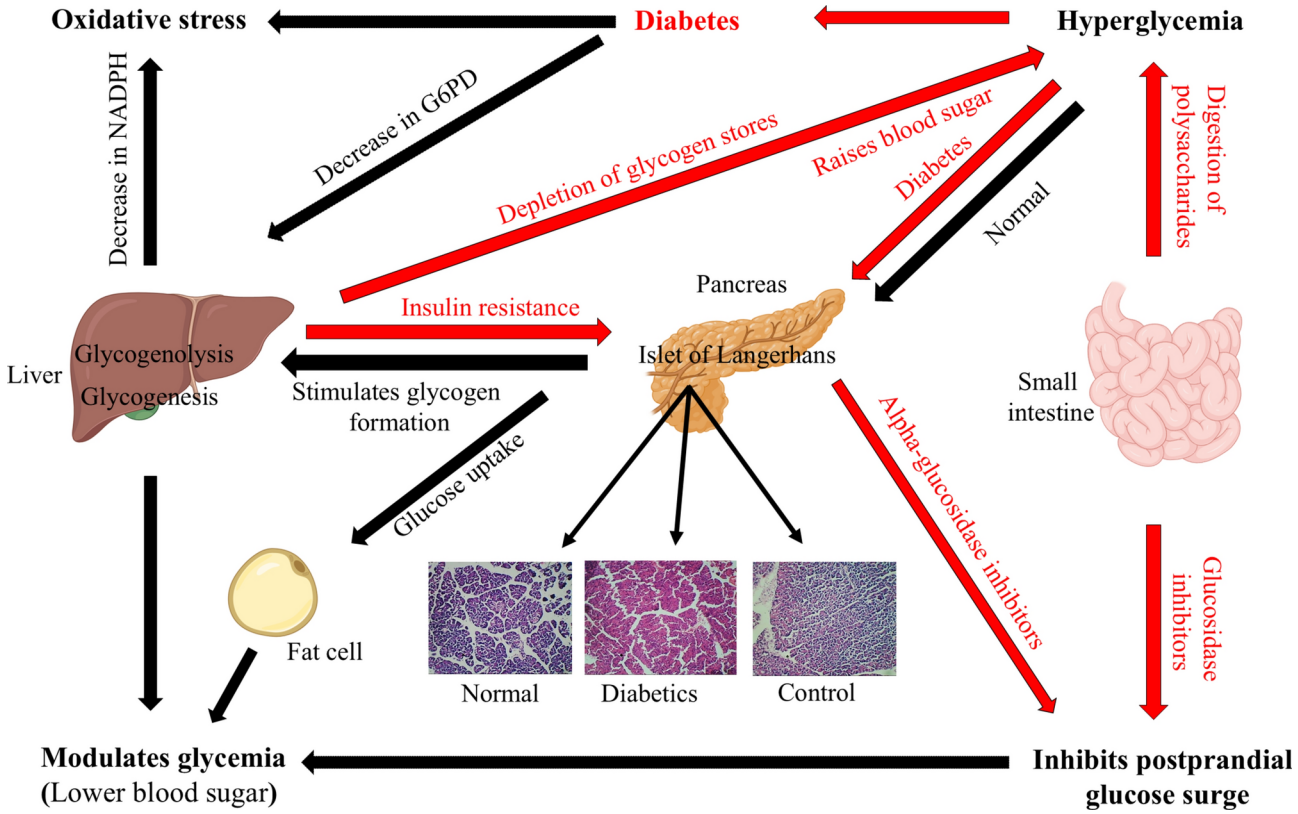

Fig. 22. Comparative diagram of glucose metabolism pathways in normal and diabetic conditions. Under normal conditions, glucose metabolism is efficiently regulated by insulin, promoting glucose uptake, glycolysis, glycogenesis, and inhibiting gluconeogenesis and lipolysis. In contrast, in diabetes, insulin resistance or deficiency disrupts glucose uptake and utilization. Leading to increased gluconeogenesis, glycogenolysis, and lipolysis, contributing to hyperglycemia and dyslipidemia. This diabetic pathway highlights oxidative stress and increased free fatty acid mobilization, underscoring the pathological shifts in metabolic balance associated with diabetes.

in the extract may have contributed to anti-inflammatory actions, reducing the inflammatory mediators that exacerbate liver damage in diabetes[105]. Overall, Medicagol and plant extracts from *C. arietinum* and *H. vulgare* exhibit strong antidiabetic potential through a combination of glycemic control, enzyme inhibition, antioxidant activity, and protection against hepatic and renal dysfunction. Natural product research is often subject to positive results bias. In this study, we prioritized a balanced presentation by critically analyzing both promising and less favorable outcomes. For example, while C. arietinum and H. vulgare extracts showed significant antidiabetic effects, other phytochemicals exhibited limited activity or demonstrated toxicity in preliminary assays. These findings highlight the need for further investigation into their safety and efficacy profiles before considering clinical applications. Toxicity assessments revealed that some phytochemicals in the tested extracts diaplayed carcinogenic potential at higher doses. This underscores the importance of rigorous toxicological evaluations to ensure the safety of these compounds. additionally, the variability in response among individual mice suggests that certain extracts may have a narrow therapeutic index, necessitating careful dose selection in future studies. These findings underscore the therapeutic promise of these phytochemicals and provide a solid foundation for further preclinical investigations into their use as natural antidiabetic agents.

Conclusion

The focus of our research was to explore the therapeutic activities of *C. arietinum* and *H vulgare*, which have been attributed to their high levels of phytochemicals. Through in-vitro analysis, we observed that C. arietinum (IC50 55.08 ± 5 µg/mL) and H. vulgare (IC50 115.8 ± 5 µg/mL) exhibit a stronger inhibitory result on α-amylase compared to the standard acarbose (IC50 196.3 ± 10 µg/mL). Additionally, both C. arietinum and H. vulgare presented potent inhibitory results beside α-glucosidase (IC50 100.2 ± 5 µg/mL and *IC50* 216.2 ± 5 µg/mL, respectively) when compared to acarbose (*IC50* 246.5 ± 10 µg/mL). In the current study, we investigated 194 active compounds found in C. arietinum and H. vulgare seeds using an in-silico approach, targeting α-amylase and α-glucosidase receptors in type 2 diabetes. In conclusion, our study provides evidence of the inhibitory effects of C. arietinum and H. vulgare extracts on α-amylase and α-glucosidase enzymes. These findings support the potential of these plant extracts as natural sources for developing antidiabetic agents. Molecular docking score designs were done, and drug-likeness and pharmacokinetic analyses were also conducted in this research.

Our virtual screening identified Medicagol, Euphol, Stigmasterol, Beta-Sitosterol, and Fucosterol as possible inhibitors of α-amylase and α-glucosidase with the high docking score and interaction for the target protein. Pharmacokinetic studies also indicated that Medicagol is a safe and non-cancerous option. However, during our molecular dynamic studies, Euphol, Stigmasterol, Beta-Sitosterol, and Fucosterol were comparatively unstable. Furthermore, in vivo investigations confirm their ability to improve glycemic control, mitigate oxidative stress, and restore pancreatic integrity in STZ-induced diabetes mice. These findings underscore the therapeutic potential of C. arietinum and H. vulgare as natural antidiabetic agents and highlight the importance of their secondary metabolites in addressing diabetes mellitus. To improve the clinical translatability of these findings, future studies should focus on: Conducting human trials to validate efficacy and safety; optimizing extraction and purification techniques to enhance bioavailability: and employing advanced omics technologies to further elucidate the molecular mechanisms underlying the antidiabetic effects of these extracts.

Data availability

The data used to support the findings of this study are available from the corresponding author upon request.

Received: 5 May 2024; Accepted: 6 February 2025
Published online: 24 February 2025

References

1. Astrup, A. Healthy lifestyles in Europe: Prevention of obesity and type II diabetes by diet and physical activity. *Public Health Nutr.* **4**(2b), 499–515 (2001).
2. Duckworth, W. C. Hyperglycemia and cardiovascular disease. *Curr. Atheroscler. Rep.* **3**(5), 383–391 (2001).
3. Cho, N. H. et al. IDF diabetes atlas: Global estimates of diabetes prevalence for 2017 and projections for 2045. *Diabetes Res. Clin. Pract.* **138**, 271–281 (2018).
4. Gao, K. et al. 1-Deoxynojirimycin: Occurrence, extraction, chemistry, oral pharmacokinetics, biological activities and in silico target fishing. *Molecules* **21**(11), 1600 (2016).
5. Thilagam, E. et al. α-Glucosidase and α-amylase inhibitory activity of Senna surattensis. *J. Acupuncture Meridian Stud.* **6**(1), 24–30 (2013).
6. Schwartz, D. D. et al. Seeing the person, not the illness: promoting diabetes medication adherence through patient-centered collaboration. *Clin. Diabetes* **35**(1), 35–42 (2017).
7. Dirir, A. M. et al. A review of alpha-glucosidase inhibitors from plants as potential candidates for the treatment of type-2 diabetes. *Phytochem. Rev.* **21**(4), 1049–1079 (2022).
8. Jia, Y., Lao, Y. & Leung, S.-W. Glycaemic control efficacy of oral antidiabetic drugs in treating type 2 diabetes: A protocol for network meta-analysis. *BMJ Open* **5**(3), e006139 (2015).
9. Mamun-or-Rashid, A. et al. A review on medicinal plants with antidiabetic activity. *J. Pharmacognosy Phytochem.* **3**(4), 149–159 (2014).
10. Wagman, A. S. & Nuss, J. M. Current therapies and emerging targets for the treatment of diabetes. *Curr. Pharm. Des.* **7**(6), 417–450 (2001).
11. Asmat, U., Abad, K. & Ismail, K. Diabetes mellitus and oxidative stress: A concise review. *Saudi Pharm. J.* **24**(5), 547–553 (2016).
12. Chaudhury, A. et al. Clinical review of antidiabetic drugs: implications for type 2 diabetes mellitus management. *Front. Endocrinol.* **8**, 6 (2017).
13. Jung, M. et al. Antidiabetic agents from medicinal plants. *Curr. Med. Chem.* **13**(10), 1203–1218 (2006).
14. Shahzad, A. et al. Flavonoids as modulators of metabolic reprogramming in renal cell carcinoma. *Oncol. Rep.* **52**(6), 167 (2024).
15. Abbasifard, M., et al. Effect of topical chickpea oil (*Cicer arietinum* L.) on knee osteoarthritis: A randomized double-blind controlled clinical trial. *Eur. J. Integr. Med.* 2020. 35: p. 101076.
16. Jukanti, A.K., et al. Nutritional quality and health benefits of chickpea (*Cicer arietinum* L.): a review. *Br. J. Nutr.*, 2012. **108**(S1): p. S11-S26.
17. Begum, N., et al. Nutritional composition, health benefits and bio-active compounds of chickpea (*Cicer arietinum* L.). *Front. Nutr.* 2023. **10**.
18. Mathew, S. E., Shakappa, D. & Rengel, Z. A review of the nutritional and antinutritional constituents of chickpea (Cicer arietinum) and its health benefits. *Crop Pasture Sci.* **73**(4), 401–414 (2022).
19. Ahmadi, N. et al. The effect of chickpea broth on knee osteoarthritis: A Pilot non-randomised open-labeled clinical study. *Adv. Integr. Med.* **7**(3), 121–125 (2020).
20. Nam, T., Kim, A. & Oh, Y. Effectiveness of chickpeas on blood sugar: A systematic review and meta-analysis of randomized controlled trials. *Nutrients* **15**(21), 4556 (2023).
21. Ramakrishna, R., et al. Phenolic linked anti-hyperglycemic bioactives of barley (Hordeum vulgare L.) cultivars as nutraceuticals targeting type 2 diabetes. Ind. *Crops Prod.* 2017. **107**, 509–517.
22. Ramnarain Ramakrishna, R. R., et al. Phenolic linked anti-hyperglycemic bioactives of barley (*Hordeum vulgare* L.) cultivars as nutraceuticals targeting type 2 diabetes. 2017.
23. Lee, N.Y., et al. Biological activity of barley (*Hordeum vulgare* L.) and barley by-product extracts. *Food Sci. Biotechnol.*, 2010; **19**: p. 785–791.
24. Zeng, Y., et al. Preventive and therapeutic role of functional ingredients of barley grass for chronic diseases in human beings. *Oxidative Med. Cell. Longevity*, 2018. **2018**.
25. Deng, L.-N., et al. Phytochemical constituents and antioxidant enzyme activity profiles of different barley (*Hordeum vulgare* L.) cultivars at different developmental stages. *Agronomy*, 2019. **10**(1), p. 37.
26. Prasad, J., et al. Effect of organic and inorganic source of nutrients on growth and yield of barley (*Hordeum vulgare* L.). *J. Pharmacognosy Phytochem.*, 2019. **8**(2), 521–523.
27. Mafakher, L., et al. Investigation of biological activities of two cultivars of Cicer arietinum proteins mass associated with Alzheimer's disease. *Proteins: Struct. Funct. Bioinform.* 2023. **91**(7): p. 859–871.
28. Sharma, S., et al. Characterization and management of Pseudomonas syringae pv. syringae, causing basal kernel blight of barley (*Hordeum vulgare* L.). *Crop Res.* 2023. **58**(1and2): p. 90–100.
29. Jebor, A. et al. Characterization and antimicrobial activity of barley grain (Hordeum vulgare) extract. *Int. J. Curr. Microbiol. Appl. Sci.* **2**(8), 41–48 (2013).
30. Yan, J.-K., et al. The anti-hyperlipidemic effect and underlying mechanisms of barley (*Hordeum vulgare* L.) grass polysaccharides in mice induced by a high-fat diet. *Food Funct.* 2023. **14**(15), 7066–7081.
31. Gul, S. et al. Multiple pathways are responsible for Anti-inflammatory and Cardiovascular activities of *Hordeum vulgare* L. *J. Translat. Med.* **12**(1), 1–8 (2014).
32. Dykes, L. & Rooney, L. Phenolic compounds in cereal grains and their health benefits. *Cereal Foods World* **52**(3), 105–111 (2007).

33. Lim, J.-M. et al. Protective effects of triple fermented barley extract (FBe) on indomethacin-induced gastric mucosal damage in rats. *BMC Complementary Altern. Med.* **19**, 1–11 (2019).
34. Lemieszek, M. K. et al. Immunomodulatory properties of polysaccharide-rich young green barley (Hordeum vulgare) extract and its structural characterization. *Molecules* **27**(5), 1742 (2022).
35. Zhu, Y., et al. Phenolics content, antioxidant and antiproliferative activities of dehulled highland barley (*Hordeum vulgare* L.). *J. Funct. Foods*, 2015. **19**, 439–450.
36. Shabbir, M. A., et al. Unraveling the role of natural functional oils in modulating osteoarthritis related complications. *Crit. Rev. Food Sci. Nutr*. 2023, 1–21.
37. Zhu, M.-X., C. Xu, and Y.P. Hao, Lactobacillus fermentation improved the nutrient value and hypoglycemic activity of chickpea milk. *Emir. J. Food Agric*. 2023.
38. Meng, Y. et al. A comparison between partially peeled hulless barley and whole grain hulless barley: Beneficial effects on the regulation of serum glucose and the gut microbiota in high-fat diet-induced obese mice. *Food Funct.* **14**(2), 886–898 (2023).
39. Kadan, S. et al. In vitro evaluation of anti-diabetic activity and cytotoxicity of chemically analysed Ocimum basilicum extracts. *Food Chem.* **196**, 1066–1074 (2016).
40. Adisakwattana, S. et al. In vitro inhibitory effects of plant-based foods and their combinations on intestinal α-glucosidase and pancreatic α-amylase. *BMC Complementary Altern. Med.* **12**(1), 1–8 (2012).
41. Kim, Y.-M., Wang, M.-H. & Rhee, H.-I. A novel α-glucosidase inhibitor from pine bark. *Carbohydr. Res.* **339**(3), 715–717 (2004).
42. Mohanraj, K. et al. IMPPAT: A curated database of I ndian M edicinal P lants, P hytochemistry A nd T herapeutics. *Sci. Rep.* **8**(1), 4329 (2018).
43. Ru, J. et al. TCMSP: A database of systems pharmacology for drug discovery from herbal medicines. *J. Cheminform.* **6**, 1–6 (2014).
44. Yadavalli, R. et al. Phytochemical screening and in silico studies of flavonoids from Chlorella pyrenoidosa. *Inform. Med. Unlocked* **10**, 89–99 (2018).
45. Rose, Y. et al. RCSB protein data bank: Architectural advances towards integrated searching and efficient access to macromolecular structure data from the PDB archive. *J. Mol. Biol.* **433**(11), 166704 (2021).
46. Saeed, M. et al. Assessment of antidiabetic activity of the shikonin by allosteric inhibition of protein-tyrosine phosphatase 1B (PTP1B) using state of art: an in silico and in vitro tactics. *Molecules* **26**(13), 3996 (2021).
47. Syaban, M. F. R. et al. Allium sativum as antimalaria agent via falciapin protease-2 inhibitor mechanism: Molecular docking perspective. *Clin. Res. J. Internal Med.* **2**(1), 130–135 (2021).
48. Mustafa, G. et al. Screening and molecular docking of selected phytochemicals against NS5B polymerase of hepatitis C virus. *Pak. J. Pharm Sci.* **33**(5), 2317–2322 (2020).
49. Cheng, F., et al. *admetSAR: A Comprehensive Source and Free Tool for Assessment of Chemical ADMET Properties*. 2012, ACS Publications.
50. Pires, D. E., Blundell, T. L. & Ascher, D. B. pkCSM: predicting small-molecule pharmacokinetic and toxicity properties using graph-based signatures. *J. Med. Chem.* **58**(9), 4066–4072 (2015).
51. Dong, J. et al. ADMETlab: A platform for systematic ADMET evaluation based on a comprehensively collected ADMET database. *J. Cheminform.* **10**, 1–11 (2018).
52. Kushwaha, P. P. et al. Phytochemicals present in Indian ginseng possess potential to inhibit SARS-CoV-2 virulence: A molecular docking and MD simulation study. *Microbial Pathogenesis* **157**, 104954 (2021).
53. Bowers, K. J., et al. Scalable algorithms for molecular dynamics simulations on commodity clusters. in *Proceedings of the 2006 ACM/IEEE Conference on Supercomputing*. 2006.
54. Azeem, M., Mustafa, G. & Mahrosh, H. S. Virtual screening of phytochemicals by targeting multiple proteins of severe acute respiratory syndrome coronavirus 2: Molecular docking and molecular dynamics simulation studies. *Int. J. Immunopathol. Pharmacol.* **36**, 03946320221142793 (2022).
55. Nath, S., Ghosh, S. K. & Choudhury, Y. A murine model of type 2 diabetes mellitus developed using a combination of high fat diet and multiple low doses of streptozotocin treatment mimics the metabolic characteristics of type 2 diabetes mellitus in humans. *J. Pharmacol. Toxicol. Methods* **84**, 20–30 (2017).
56. Wang-Fischer, Y. & Garyantes, T. Research article improving the reliability and utility of streptozotocin-induced rat diabetic model. *Age (Weeks)* **6**(11), 12–17 (2018).
57. Xu, W. et al. Anti-diabetic effects of polysaccharides from Talinum triangulare in streptozotocin (STZ)-induced type 2 diabetic male mice. *Int. J. Biol. Macromol.* **72**, 575–579 (2015).
58. Parker, K. *The Role of the Intestinal Immune System in the Development and Treatment of Type 2 Diabetes* (Stellenbosch University, 2022).
59. Kandouli, C. et al. Antidiabetic, antioxidant and anti inflammatory properties of water and n-butanol soluble extracts from Saharian Anvillea radiata in high-fat-diet fed mice. *J. Ethnopharmacol.* **207**, 251–267 (2017).
60. Jayachandran, M. et al. Isoquercetin ameliorates hyperglycemia and regulates key enzymes of glucose metabolism via insulin signaling pathway in streptozotocin-induced diabetic rats. *Eur. J. Pharmacol.* **829**, 112–120 (2018).
61. Parveen, K. et al. Protective effects of Pycnogenol® on hyperglycemia-induced oxidative damage in the liver of type 2 diabetic rats. *Chemico-Biol. Interact.* **186**(2), 219–227 (2010).
62. Du, S. et al. Biological investigations on therapeutic effect of chitosan encapsulated nano resveratrol against gestational diabetes mellitus rats induced by streptozotocin. *Drug Delivery* **27**(1), 953–963 (2020).
63. Srinivasan, S. & Pari, L. Ameliorative effect of diosmin, a citrus flavonoid against streptozotocin-nicotinamide generated oxidative stress induced diabetic rats. *Chemico-Biol. Interactions* **195**(1), 43–51 (2012).
64. Gutierrez, J. C. et al. Aortic and ventricular dilation and myocardial reduction in gestation day 17 ICR mouse fetuses of diabetic mothers. *Birth Defects Res. Part A: Clin. Mol. Teratology* **79**(6), 459–464 (2007).
65. Chatterjee, S., Khunti, K. & Davies, M. J. Type 2 diabetes. *Lancet* **389**(10085), 2239–2251 (2017).
66. Mechchate, H. et al. In vitro alpha-amylase and alpha-glucosidase inhibitory activity and in vivo antidiabetic activity of Withania frutescens L. Foliar extract. *Molecules* **26**(2), 293 (2021).
67. Roshni, J., et al. Multi-target potential of Indian phytochemicals against SARS-CoV-2: A docking, molecular dynamics and MM-GBSA approach extended to Omicron B. 1.1. 529. *J. Infect. Public Health*, 2022. **15**(6), 662–669.
68. Zhang, D. et al. Based on network pharmacology and molecular docking, the active components, targets, and mechanisms of Flemingia Philippinensis in improving inflammation were excavated. *Nutrients* **16**(12), 1850 (2024).
69. Kavalalı, G. et al. Hypoglycemic activity of Urtica pilulifera in streptozotocin-diabetic rats. *J. Ethnopharmacol.* **84**(2–3), 241–245 (2003).
70. Bender, D. A. and Mayes, P. A. *The Pentose Phosphate Pathway and & Other Pathways of Hexose Metabolism*. Harper's Illustrated Biochemistry. 31st ed. McGraw-Hill Education, New York, 2018: 452–473.
71. Mayes, P. A. and Bender, D. A. *The Pentose Phosphate Pathway & Other Pathways of Hexose Metabolism*. A LANGE Medical Book, 2003: p. 163.
72. Xu, Y. et al. Glucose-6-phosphate dehydrogenase-deficient mice have increased renal oxidative stress and increased albuminuria. *FASEB J.* **24**(2), 609 (2010).
73. Nóbrega-Pereira, S. et al. G6PD protects from oxidative damage and improves healthspan in mice. *Nature Commun.* **7**(1), 10894 (2016).

74. Tanabe, K. et al. Genetic deficiency of glycogen synthase kinase-3β corrects diabetes in mouse models of insulin resistance. *PLoS Biology* **6**(2), e37 (2008).
75. Mir-Coll, J. et al. Genetic models rule out a major role of beta cell glycogen in the control of glucose homeostasis. *Diabetologia* **59**(5), 1012–1020 (2016).
76. Liu, Y. et al. Conditional ablation of Gsk-3β in islet beta cells results in expanded mass and resistance to fat feeding-induced diabetes in mice. *Diabetologia* **53**, 2600–2610 (2010).
77. Ennulat, D. et al. Diagnostic performance of traditional hepatobiliary biomarkers of drug-induced liver injury in the rat. *Toxicol. Sci.* **116**(2), 397–412 (2010).
78. Bailey, W. J. et al. A performance evaluation of three drug-induced liver injury biomarkers in the rat: alpha-glutathione S-transferase, arginase 1, and 4-hydroxyphenyl-pyruvate dioxygenase. *Toxicol. Sci.* **130**(2), 229–244 (2012).
79. Hernández, A. F. et al. Pesticide exposure and genetic variation in xenobiotic-metabolizing enzymes interact to induce biochemical liver damage. *Food Chem. Toxicol.* **61**, 144–151 (2013).
80. Lozano-Paniagua, D. et al. Evaluation of conventional and non-conventional biomarkers of liver toxicity in greenhouse workers occupationally exposed to pesticides. *Food Chem. Toxicol.* **151**, 112127 (2021).
81. Nunes, C.d.R., et al., *Plants as sources of anti-inflammatory agents.* Molecules, 2020. **25**(16): p. 3726.
82. Kuznetsova, V. Y., Kravchenko, V., and Seniuk, I. *Important Advantages of Phenolic Components of Plant Origin for Pharmacocorrection of Pathological States.* 2024.
83. Yatoo, M. I. et al. Anti-inflammatory drugs and herbs with special emphasis on herbal medicines for countering inflammatory diseases and disorders-a review. *Recent Patents Inflammation Allergy Drug Discovery* **12**(1), 39–58 (2018).
84. Ozbek, E. Induction of oxidative stress in kidney. *Int. J. Nephrol.* **2012**(1), 465897 (2012).
85. Vaziri, N. D. & Rodríguez-Iturbe, B. Mechanisms of disease: oxidative stress and inflammation in the pathogenesis of hypertension. *Nature Clin. Pract. Nephrol.* **2**(10), 582–593 (2006).
86. Schofield, J. D. et al. Diabetes dyslipidemia. *Diabetes Therapy* **7**, 203–219 (2016).
87. Wu, L. & Parhofer, K. G. Diabetic dyslipidemia. *Metabolism* **63**(12), 1469–1479 (2014).
88. Czech, M. P. et al. Insulin signalling mechanisms for triacylglycerol storage. *Diabetologia* **56**, 949–964 (2013).
89. Herrera, E. & Ortega-Senovilla, H. Disturbances in lipid metabolism in diabetic pregnancy–are these the cause of the problem?. *Best Pract. Res. Clin. Endocrinol. Metab.* **24**(4), 515–525 (2010).
90. Kardum, N. and Glibetic, M. Polyphenols and their interactions with other dietary compounds: Implications for human health, in *Advances in Food and Nutrition Research*. 2018, Elsevier. p. 103–144.
91. Derosa, G. et al. Lipid-lowering nutraceuticals update on scientific evidence. *J. Cardiovasc. Med.* **21**(11), 845–859 (2020).
92. Newsholme, P. et al. Molecular mechanisms of ROS production and oxidative stress in diabetes. *Biochem. J.* **473**(24), 4527–4550 (2016).
93. Tangvarasittichai, S. Oxidative stress, insulin resistance, dyslipidemia and type 2 diabetes mellitus. *World J. Diabetes* **6**(3), 456 (2015).
94. Vanessa Fiorentino, T. et al. Hyperglycemia-induced oxidative stress and its role in diabetes mellitus related cardiovascular diseases. *Curr. Pharm. Des.* **19**(32), 5695–5703 (2013).
95. Lima, J. E., Moreira, N. C. & Sakamoto-Hojo, E. T. Mechanisms underlying the pathophysiology of type 2 diabetes: From risk factors to oxidative stress, metabolic dysfunction, and hyperglycemia. *Mutation Res./Genet. Toxicol. Environ. Mutagenesis* **874**, 503437 (2022).
96. Singh, A. et al. Mechanistic insight into oxidative stress-triggered signaling pathways and type 2 diabetes. *Molecules* **27**(3), 950 (2022).
97. Kutan Fenercioglu, A. et al. The effects of polyphenol-containing antioxidants on oxidative stress and lipid peroxidation in Type 2 diabetes mellitus without complications. *J. Endocrinol. Investig.* **33**, 118–124 (2010).
98. Chaiyasut, C. et al. Effects of phenolic compounds of fermented Thai indigenous plants on oxidative stress in streptozotocin-induced diabetic rats. *Evid.-Based Complementary Alternative Med.* **2011**(1), 749307 (2011).
99. Krawczyk, M. et al. Impact of polyphenols on inflammatory and oxidative stress factors in diabetes mellitus: Nutritional antioxidants and their application in improving antidiabetic therapy. *Biomolecules* **13**(9), 1402 (2023).
100. Madić, V. et al. Polyherbal mixture ameliorates hyperglycemia, hyperlipidemia and histopathological changes of pancreas, kidney and liver in a rat model of type 1 diabetes. *J. Ethnopharmacol.* **265**, 113210 (2021).
101. Dall'Asta, M., et al. Protection of pancreatic β-cell function by dietary polyphenols. *Phytochem. Rev.* 2015. **14**, 933–959.
102. Tarasiuk, A. & Fichna, J. Effectiveness and therapeutic value of phytochemicals in acute pancreatitis: A review. *Pancreatology* **19**(4), 481–487 (2019).
103. Dkhil, M. A. et al. Chlorogenic acid prevents hepatotoxicity in arsenic-treated mice: role of oxidative stress and apoptosis. *Mol. Biol. Rep.* **47**, 1161–1171 (2020).
104. Alsharif, K. F. et al. Melatonin downregulates the increased hepatic alpha-fetoprotein expression and restores pancreatic beta cells in a streptozotocin-induced diabetic rat model: A clinical, biochemical, immunohistochemical, and descriptive histopathological study. *Front. Vet. Sci.* **10**, 1214533 (2023).
105. Lucchesi, A. N., Cassettari, L. L. & Spadella, C. T. Alloxan-induced diabetes causes morphological and ultrastructural changes in rat liver that resemble the natural history of chronic fatty liver disease in humans. *J. Diabetes Res.* **2015**(1), 494578 (2015).

Acknowledgements

We extend our sincere gratitude to Dr. Muhammad jangheer, Department of Biochemistry, Government College University Faisalabad, Pakistan for his invaluable assistance with the in-vivo analysis. We also acknowledge Mr. Muhammad Javed Iqbal, Department of Zoology, Government College University Faisalabad, Pakistan for his significant contribution to the enzymatic inhibition assays. Their support and expertise greatly enhanced the quality and scope of this research. We express our sincere gratitude to the International Education School (IES), Kunming Medical University, China for providing a conducive academic environment and the necessary resources to carry out this research.

Author contributions

QZ and ZY were responsible for the entire experiment design. Enzymatic assay, in vivo analysis and statical analysis were performed with the help of WL, YN, KC, YS, XL, QD, JX, JZ, ZX, BS, and YZ. As and SH analyzed bioinformatics assay. As and QZ checked all results, organized figures, and wrote the manuscript. All authors checked and approved the final version of this manuscript.

Funding

This work was supported by the National Natural Science Foundation of China (No. 82460510, 82203565, 82103388, and 31960145), Yunnan province applied research funds (202201AY070001-011, 202201AY070001-

043, and 202201AS070077) and Science and technology innovation team of tumor metabolism research, Kunming Medical University (CXTD202102).

Declarations

Competing interests
The authors declare no competing interests.

Additional information
Correspondence and requests for materials should be addressed to Q.Z. or Z.Y.

Reprints and permissions information is available at www.nature.com/reprints.

Publisher's note Springer Nature remains neutral with regard to jurisdictional claims in published maps and institutional affiliations.